Journal of Medicinal Chemistry

Article

Full sequence amino acid scanning of #-defensin RTD-1 yields a potent anthrax lethal factor protease inhibitor

Yilong Li, Andrew Gould, Teshome Aboye, Tao Bi, Leonard M. Breindel, Alexander Shekhtman, and Julio A. A Camarero

J. Med. Chem., **Just Accepted Manuscript** • DOI: 10.1021/acs.jmedchem.6b01689 • Publication Date (Web): 02 Feb 2017

Full sequence amino acid scanning of θ-defensin RTD-1 yields a potent anthrax lethal factor protease inhibitor

Yilong Li[1], Andrew Gould[1], Teshome Aboye[1], Tao Bi[1], Leonard Breindel[3], Alexander Shekhtman[3] and Julio A. Camarero[1,2*]

[1]Department of Pharmacology and Pharmaceutical Sciences and [2]Department of Chemistry, University of Southern California, Los Angeles, CA 90089-9121, USA; [3]Department of Chemistry, State University of New York, Albany, NY 12222, USA

ABSTRACT. θ-Defensin RTD-1 is a non-competitive inhibitor of anthrax lethal factor (LF) protease (IC_{50} = 390 ± 20 nM, K_i = 365 ± 20 nM) and a weak inhibitor of other mammalian metalloproteases such as TNFα converting enzyme (TACE) (K_i = 4.45 ± 0.48 μM). Using full sequence amino acid scanning in combination with a highly efficient 'one-pot' cyclization-folding approach we obtained an RTD-1 based peptide that was around 10-times more active than wild type RTD-1 in inhibiting LF protease (IC_{50} = 43 ± 3 nM, K_i = 18 ± 1 nM). The most active peptide was completely symmetrical, rich in Arg and Trp residues, and able to adopt a native RTD-1-like structure. These results show the power of optimized chemical peptide synthesis approaches for the efficient production of libraries of disulfide-rich backbone-cyclized peptides to quickly perform structure-activity relationship studies for optimizing protease inhibitors.

INTRODUCTION

Defensins are cysteine-rich antimicrobial peptides that are important in the innate immune defense of mammals.[1-3] Defensins are classically known for their antimicrobial activities, but they have been also shown to be involved in other defense mechanisms including immune modulation, neutralization of endotoxins, and anti-cancer properties.[3, 4] Mammalian defensins are positively charged peptides containing mostly β-sheet structures and six conserved cysteines forming three intramolecular disulfides. They can be classified into α-, β- and θ-defensins depending on their overall structure.

The overall fold of α and β-defensins is very similar except for the disulfide connectivities, and the presence of an N-terminal α-helix segment in β-defensins that is missing in α-defensins.[5] In contrast, θ-defensins are backbone cyclized peptides formed by the head-to-tail covalent assembly of two polypeptides derived from α-defensin related precursors.[1] Although the mechanism for RTD-1 processing still remains unclear, it is regarded to involve two dodecapeptides, each containing a three residue C-terminal pro-sequence.[1] θ-Defensins are to date the only known cyclic polypeptides expressed in animals.[1]

Rhesus θ-defensin-1 (RTD-1) was the first θ-defensin to be discovered from an extract of Rhesus macaques leukocytes.[1] Defensin RTD-1, unlike α- and β-defensins, possesses a β-hairpin-like structure with two anti-parallel β-strands stabilized by three disulfides in a ladder configuration (**Fig. 1**).[6] Other less abundant RTD variants have been named RTD-2 to RTD-6, have also been found in Rhesus macaques.[7-9] Circular θ-defensins have also been found in other primate species.[10-12] Intriguingly, although humans possess genes encoding θ-defensins, the ability to produce these cyclic defensins have been lost due to a stop codon mutation within the signal sequence, which prevents subsequent translation.[13]

θ-Defensins have antimicrobial activity against both Gram-positive and Gram-negative bacteria,[1] The antibacterial activity, however, has been shown to strongly depend on the experimental conditions, mostly buffer composition and presence of serum proteins, used in the antibacterial assays.[14] θ-Defensins also have anti-fungal[1] and anti-HIV[13, 15] activities. Chemically-synthesized human θ-defensins (also called retrocyclins), which are derived from the human pseudogene sequences, have been shown to protect human cells from infection by HIV-1[13] and have been evaluated as a topical anti-HIV agent.[16-18] θ-Defensins have also been shown to inactivate germinating anthrax spores and act as a non-competitive inhibitor of anthrax lethal factor (LF) protease and other metalloproteases like TNFα converting enzyme (TACE).[19] Due to its network of disulfide bonds and backbone-cyclized topology θ-defensins present high resistance to proteolytic degradation in serum and plasma.[20] θ-Defensins have been shown to possess anti-inflammatory properties in animal models.[20] Altogether, these data suggest that the θ-defensin is an ideal molecular framework for the development of novel peptide-based therapeutics.[20, 21]

We have recently developed a method for the rapid parallel production of disulfide-rich backbone cyclized polypeptides using a 'tea-bag' approach in combination with high efficient cyclization-folding protocols.[22, 23] This approach has been recently used for the production of cyclotide-based amino acid scanning libraries.[23] We decided to use this approach for the rapid production of a full sequence amino acid scanning library on defensin RTD-1 in order to improve its inhibitory activity against the protease LF that was used as a model. LF is a Zn^{+2}-dependent metalloprotease that cleaves several mitogen-activated protein kinases and is responsible for the lethality of anthrax lethal toxin [24] and therefore is a validated molecular target for the development of more efficient therapeutics to treat anthrax.[25]

In general, all the positions in RTD-1 were amenable to mutation with exception of the Arg residues located in the β-sheet region of the peptide. Replacement of these residues by non-

charged residues yielded cyclic peptides that were unable to fold correctly. The anti-LF activity of all the folded cyclic peptides was evaluated *in vitro* using a fluorogenic reporter. We found that the native Arg residues in RTD-1 are key for anti-LF activity. Mutation of these residues to negatively charged amino acids significantly decreased the anti-LF activity of the resulting peptides. Mutation of the non-hydrophobic native residues located in the loops of RTD-1 to Arg also resulted in peptides with improved biological activity. In addition, we observed that the replacement of hydrophobic residues by Trp also increased the anti-LF activity. Combining this information we were able to produce a natively folded RTD-1-based backbone cyclized polypeptide that was about 10 times more active than native RTD-1. These results highlight the power of optimized chemical cyclization/folding techniques for the rapid production of positional scanning libraries, which can be quickly used to perform structure activity relationship studies for improving the biological activity of bioactive peptides.

RESULTS

Peptide library design

Every residue in the sequence of RTD-1, except for the cysteines that are required for disulfide formation and oxidative folding, was systematically replaced by a set of amino acids containing small (Ala), hydrophobic (Leu, Ile or Val), aromatic (Tyr or Trp), positively (Arg, Lys or His) or negatively (Asp or Glu) charged residues to provide a total of 12 sub-libraries with the objective to evaluate the importance of every native residue for the anti-LF activity of RTD-1 (**Fig. 1**). Each amino acid position was scanned with 9 residues (except position 2 that was scanned with only 8 residues) from the different groups described above. Therefore, positions in RTD-1 were replaced by a set of amino acids containing Ala, Asp, Glu, Leu, Val, Lys, Arg, Tyr or Trp. When the native the residue on the RTD-1 sequence was Arg, Leu, or Val, the corresponding amino acid in the set indicated above was replaced by His (Arg) or Ile (Val and Leu). The residue Leu was not

included in the Phe2 sub-library therefore this sub-library contained only 8 members. Accordingly, a total of 107 (=11 x 9 + 1 x 8) different f RTD-1 variants containing a single mutation were chemically prepared (**Table S1**). Wild-type RTD-1 was also included in the study as a positive control. In addition, the disulfide-free cyclic form of the θ-defensin, RTD-1 C3S, C5S, C12S, C14S, C16S (RTD-1-C*S) (**Table S1**), was also used to evaluate the importance of the disulfide network for the anti-LF activity of defensin RTD-1.

Peptide synthesis

All the cyclic single mutant variants of defensin RTD-1 (**Table S1**) were chemically synthesized employing Fmoc-based solid-phase peptide synthesis on a sulfonamide resin[26-28] and a 'tea-bag' approach (**Fig. 2**).[23] We used the peptide bond between residues Leu6 and Cys7 as the cyclization site for most of the positional scanning libraries except for the R4 and L6 sub-libraries, where the peptide bond between residues Phe2 and Cys3 was used instead. Both cyclization sites have shown to provide very good cyclization yields in the synthesis of RTD-1.[22] The synthesis of the common C-terminal sequence for all the cyclic RTD-1 sub-libraries was performed at 0.1 mmol scale on an automated peptide synthesizer ABI433A. When the position to be scanned was reached for a particular sub-library, the resin was divided in 9 equimolar aliquots containing around 11 μmol each (**Fig. 2**). Each resin was manually coupled in parallel with the corresponding activated Fmoc-amino acid derivative. Once the couplings were complete, each resin was placed in an individual sealed poly-propylene 'tea-bag' (measuring around 30 x 20 mm), properly tagged for identification and the synthesis was continued on the synthesizer using the ABI433A 0.25 mmol scale reaction vessel, which has a capacity of 42 mL (**Fig. 2**). This reaction vessel was able to accommodate up to 9 'tea-bags' with the dimensions described above. The number of 'tea-bags', however, could likely be easily increased by using smaller 'tea-bags' to increase the number of amino acids used in particular position of the

sequence. Once the synthesis of all the RTD-1 linear precursor analogs was complete, activation of the corresponding peptide sulfonamide-resins was performed in parallel with iodoacetonitrile, followed by cleavage with ethyl mercaptoacetate and acidolytic deprotection provided the fully deprotected linear peptide α-thioester precursors (**Fig. 2**). The peptide crudes were characterized by HPLC and electrospray mass spectrometry (ES-MS) and in all the cases the major product was the corresponding linear precursor thioester (**Fig. 3**).

Peptide cyclization/folding and purification

The corresponding peptide thioester precursors were directly cyclized and folded in parallel in a 'one-pot' reaction using sodium phosphate buffer at pH 7.2 in the presence of 1 mM glutathione (GSH). Under these conditions defensin RTD-1 has been shown to cyclize and adopt a native θ-defensin fold as determined by NMR.[22] The cyclization/folding reactions were followed by HPLC and shown to be complete in 24–48 h. As previously reported the cyclization of RTD-1 under these conditions provided a very clean reaction crude where the natively folded defensin was the major product (≈90% by HPLC) (**Fig. 3**). The control peptide **1** (RTD-1 C*S), which has all native Cys residues mutated to Ser except Cys7, also showed an efficient backbone cyclization (**Fig. S8**). This result suggests that the presence of disulfides is not required for the effective chemical cyclization of the RTD-1 linear precursors when performed *in vitro* using an intramolecular version of native chemical ligation and therefore that the backbone cyclization in RTD-1 is likely not driven by the formation of the native disulfide network. It is important to note, however, that as the mechanism for the biosynthesis of RTD-1 remains unclear, the *in vivo* processing of θ-defensins may still rely on prior formation of the cysteine ladder.

Most of the RTD-1 single mutants were able to cyclize and fold with yields similar to that of wild-type RTD-1 (≈80-90%), and only the non-charged mutants in the R4 and R13 sub-libraries failed to fold correctly under the conditions described above providing in all cases a complex

cyclization/folding crude (**Fig. S1**). Complete chemical reduction of these crudes showed a major product that was identified by ES-MS as the corresponding fully reduced backbone cyclized polypeptide (**Fig. S2**). These results indicate that these mutations, while allowing cyclization, were unable to produce a major folded product. Intriguingly, replacement of these Arg residues by either positively (Lys or His) or negatively (Asp or Glu) charged residues provided very clean cyclization/folding crudes in all the cases (**Fig. S1**).

Given the relatively high purity of majority of the cyclization/folding crudes, most of the RTD-1 single mutants were desalted using a C18 cartridge solid phase extraction (SPE) to remove the buffer components. Only mutants R8L and V11E were purified by C18 reverse-phase HPLC (**Fig. S3**).

Biological activity of single RTD-1 mutants against lethal factor protease

To evaluate the effect of the different mutations on the biological activity of the corresponding θ-defensin analogs, we tested the ability of all the single mutant RTD-1-based peptides to inhibit the metalloprotease lethal factor using a FRET-based fluorogenic substrate.[29] This FRET-based reporter was designed to contain a LF recognition sequence flanked by the FRET pair formed by CyPet and YPet fluorescent proteins (**Figs. 4** and **S4**). The cyclic defensin RTD-1 was able to inhibit metalloprotease LF in a dose dependent manner with an IC_{50} value of 390 ± 20 nM (K_i = 365 ± 20 nM) and Hill-slope of -1.1 ± 0.1 (**Fig. 4**). On the other hand, the disulfide free form of RTD-1 (peptide **1**) did not show any activity up to 10 μM, therefore indicating that the folded structure of RTD-1 is required for LF inhibitory activity (**Fig. 4A**). All the RTD-1 mutants tested were also able to inhibit LF in a dose dependent manner with IC_{50} values ranging from 6.4 ± 0.7 μM (RTD-1 R4D) to 198 ± 26 nM (RTD-1 V11W, peptide **7**) and an average Hill slope of -1.0 ± 0.2 (**Figs. 4** and **S4**). These data suggest that these RTD-1 analogs were correctly folded and that the molecular stoichiometry of the inhibitory reaction is 1:1.

The relative activities of all the single mutants that were able to provide a single folded product are summarized in **Fig. 4B**. θ-Defensin RTD-1 is highly rich in positively charged (≈30% of residues are Arg) and hydrophobic/aromatic (≈ 22% of residues are Phe, Leu, Val or Ile) residues. In general, the introduction of negatively charged residues (Asp or Glu) reduced the inhibitory activity of resulting RTD-1 analogs. This effect was more apparent when the mutations were affecting native Arg residues on the sequence of RTD-1. For example, mutations R4E, R8E, R9E and R13E mutants showed only from 8% to 29% of the original activity of RTD-1. Similar reduction in activity was observed when Arg residues were mutated to Asp. Introduction of negatively charged residues in other positions also had a negative effect on the biological activity although the results were not that pronounced with the biological activity ranging from ≈14% (F2 position) to ≈57% (average for G1 and G10 positions) of that of RTD-1 (**Fig. 4B**). Replacing Arg residues by positively charged residues (Lys or His) also produced less active RTD-1 analogs, with activities ranging from ≈41% (average for positions R4 and R13) to ≈75% (average for R9 and R18 positions), hence highlighting the importance of the Arg residues for anti-LF activity. Introduction of positive charged (Lys or Arg) residues in non-hydrophobic positions had in general a positive effect on the activity (**Fig. 4B**). Introduction of Arg in positions G1, G10 and T17 gave RTD-1 analogs with activities ranging from 114% (T17 position) to ≈138% (average for G1 and G10 positions) of that of wild-type RTD-1. The effect was slightly less marked when these positions were mutated to Lys.

In general, the mutation of the native hydrophobic/aromatic residues (F2, L6 and I15 positions) present in the sequence of RTD-1 by positive or negatively charged residues had a detrimental effect on the activity of the resulting mutants (**Fig. 4B**). Intriguingly, replacement of the V11 position by either Lys or Arg residues had practically no effect on the biological activity of the resulting mutants. The introduction of Trp in the L6, V11 and I15 positions, however, yielded

mutants with significant better activity than that of wild-type RTD-1. For example, RTD-1 V11W (peptide **7**) and RTD-1 I15W had both around 183% of RTD-1 anti-LF activity, while mutant RTD-1 L6W (peptide **2**) had around 176% of the RTD-1 activity. Replacement of Phe at position 2 of RTD-1 by any amino acid besides Trp was detrimental for the biological activity, while the RTD-1 F2W mutant had basically the same activity than RTD-1 (**Fig. 4B**).

Since mutants R8L and RTD-1 V11E were purified by HPLC, we decided to compare the anti-LF activity of the corresponding desalted cyclization/folding crudes with the purified peptides. The biological activities in both cases were almost identical within the experimental error (**Fig. S3**). For peptide RTD-1 R8L, the IC_{50} values of the desalted crude and purified peptide were 505 ± 59 nM and 558 ± 55 nM, respectively.

Design of RTD-1 analogs with multiple mutations

Encouraged by these results we decided to explore if the effects seen with individual mutations were additive. Accordingly, we designed a total of six RTD-1 analogs containing multiple mutations that were shown to be positive for the anti-LF biological activity (**Fig. 5A**). The six RTD-1 analogs (peptides **8** through **13**, **Fig. 5A**) were chemically synthesized as described previously. The 'one-pot' backbone cyclization/folding was also very efficient in all the cases. Due to the low number of analogs, we decided to purify them by C18-reversed phase HPLC to provide high purity peptides for biological and structural assays (**Fig. S5**). The different RTD-1 analogs were tested for anti-LF activity as described before. In all cases the peptides inhibited LF in a dose dependent manner, showed Hill-slopes close to -1 and showed better activities than the best of the single mutation RTD-1 analogs, mutant V11W (peptide **7**, IC_{50} =197 ± 26 nM) (**Fig. 5**). Analog **8**, which contains mutations G10R and V11W located in one of the loops of RTD-1, was around three times more potent than RTD-1 (IC_{50} = 125 ± 15 nM). Peptide **8** was more active than the single mutants G10R (peptide **4**, IC_{50} = 262 ± 24 nM) and V11W (peptide **7**, IC_{50}

=197 ± 26 nM) indicating some degree of cooperativity between these two mutations. Analog **9** included a third mutation (L6W) located in the β-sheet region of RTD-1. This defensin was around four times more potent than wild-type RTD-1 with an IC_{50} value of 92 ± 10 nM. Peptide **10** added a fourth mutation (L6W), also located in the β-sheet region of RTD-1. The activity of this peptide (IC_{50} = 100 ± 10 nM) was similar to that of analog **9**.

At this point and given the pseudo-symmetry of RTD-1 we decided to explore adding similar mutations to the other loop of RTD-1. θ-Defensin **11** contained the additional mutation F2W providing an analog that was about five times more potent than RTD-1 (IC_{50}= 83 ± 7 nM). Adding mutations G1R (peptide **12**) and G1R,T17R (peptide **13**) further improved the biological activity of the resulting defensins by around six and ten times, respectively, when compared to that of the wild-type RTD-1 peptide (IC_{50} = 61 ± 6 and 43 ± 3 nM, respectively) (**Fig. 5**). The K_i value for peptide **13** against LF protease was estimated to be 18 ± 1 nM.

Inhibitory activity of RTD-1 mutants against metalloprotease TNFα converting enzyme (TACE)

We decided to test the selectivity of the most active RTD-1 based defensins against TACE. TACE is a member of the ADAM (a disintegrin and metalloproteinase) family, which is also known as ADAM17.[30, 31] TACE is the proteolytic enzyme that processes the membrane-bound TNFα precursor into soluble TNFα. Since TNFα is a pro-inflammatory cytokine that plays an important role in inflammatory process in many immune-mediated disorders and cancer, TACE has become a molecular target for anti-inflammatory therapies.[32, 33]

We used a fluorogenic peptide substrate to test the activity of the different RTD-1 mutants. Initial studies were done using the catalytic domain of TACE, fragment 223-474. Wild-type RTD-1, however, failed to inhibit the proteolytic activity of TACE (223-474). In contrast, RTD-1 was able to inhibit in a dose-dependent fashion and a Hill-slope of -1.0 ± 0.1 the whole extracellular domain of TACE (fragment 223-671), although with a relatively modest activity (IC_{50} = 4.5 ± 0.5

μM) (**Table 1** and **Fig. S6**). These data suggest that RTD-1 is a modest non-competitive inhibitor of TACE. Under the conditions used in the inhibitory assay the K_i value was estimated to be similar to the IC_{50}.

Next we investigated the activity of some the single mutant RTD-1 analogs. Again, all the mutants analyzed were able to inhibit TACE in a in a dose-dependent fashion and a Hill-slope around -1.0 (**Table 1** and **Fig. S6**). For example, introduction of mutations L6D and G10D in RTD-1, peptides **3** and **5** (Table 1), were able to improve around four times the biological activity against TACE, while the same mutations had a significant detrimental effect on the activity against LF, around 3-4 times less active than wild-type RTD-1 (**Table 1** and **Fig. S6**). Intriguingly, introduction of mutation V11W (peptide **7**) produced a significant increase in anti-TACE activity of the corresponding mutant, about 25 times more potent than RTD-1 (IC_{50} = 175 ± 19 nM), while the same mutation had only a modest effect on anti-LF activity (**Table 1** and **Fig. S7**). In contrast with LF protease, the addition of additional mutations had a detrimental effect on the anti-TACE activity. For example analogs **8** and **9**, both containing the additional mutations G10R and G10R/L6W, respectively, were about 4 times less potent than the single mutant V11W peptide **7** (**Table 1**). Furthermore, peptide **13**, which contains multiple mutations and is the most active RTD-1 analog against LF (K_i = 18 ± 1 nM), was only a modest inhibitor for TACE (K_i =1.20 ± 0.15 μM) being around 7 times less potent than the single mutant V11W (peptide **7**). Altogether, these data indicate that θ-defensin analog **13** is a selective and more potent LF inhibitor than RTD-1.

P□□□□□□□ 13 is a specific inhibitor of LF

To eliminate the possibility of non-specific inhibition, the most active RTD-1 analog (peptide **13**) was also tested in the presence of 1 mg/mL bovine serum albumin (BSA) (≈ 15 μM) (**Table 1**). The use of BSA at this concentration is widely used in high throughput screening assays to avoid

the selection on non-specific inhibitors.[34, 35] Under these conditions, θ-defensins RTD-1 and **13** were able to inhibit LF in a dose-dependent fashion with a IC_{50} values of 1.06 ± 0.14 and 250 ± 39 nM, respectively (**Table 1** and **Fig. S7**). In contrast, this peptide did not show any activity against TACE under these conditions (IC_{50} ≥ 10 μM) (**Table 1** and **Fig. S7**). The single mutant V11W (peptide **7**) was also able to inhibit the enzyme TACE in the presence of BSA in a dose-dependent. However, it was only a modest inhibitor under these conditions with an IC_{50} value of 3.08 ± 0.50 μM (**Table 1** and **Fig. S7**). These results strongly indicate that peptide **13** is a specific inhibitor for LF protease.

P□□□□□□□ 13 is not toxic to mammalian cells

Due to the high content of Arg and Trp residues in peptide **13**, we decided to evaluate the cytotoxicity of this peptide against mammalian cells. Trp and Arg residues possess some key chemical properties that make them ideal components for peptides able to interact and interfere with the biological activity of cellular membranes. For example, Arg residues provide the peptides with cationic charges and hydrogen bonding properties necessary for interaction with the abundant anionic components of cellular membranes, while Trp has a distinct preference for interacting with the interfacial region of lipid bilayers. In addition, Arg and Trp residues can interact through cation–π interactions, thereby facilitating enhanced peptide–membrane interactions.

The cytotoxicity of peptides **13** and RTD-1 (used as control) was tested against HeLa cells using an MTT assay. Under these conditions none of the peptides show any cellular toxicity at concentrations up to 100 μM (**Fig. S13**)

Peptide 13 adopts a native θ-defensin fold

Cyclic peptide **13** was fully characterized by NMR (**Figs. 6** and **S10**, and **Table S2**). The NMR spectrum of **13** was monodispersed showing a single conformation in solution. The ^{15}N-HSQC

spectrum of uniformly ^{15}N labeled [*U*- ^{15}N] **13** was relatively simple and well dispersed in the amide proton region, indicating a folded structure and a high degree of structural symmetry (**Fig. 6A**, see also **Fig. S10**). The indole and backbone NH cross-peaks for all the Trp residues and backbone and guanidino NH cross-peaks for residues Arg4, Arg8, Arg12, and Arg17 were highly clustered around 10 ppm (^{1}H)/129 ppm (^{15}N), 9.2 ppm (^{1}H)/125 ppm (^{15}N), 8.6 ppm (^{1}H)/122.5 ppm (^{15}N), and 7.1 ppm (^{1}H)/116.5 ppm (^{15}N) , respectively (**Fig. 6A**). The backbone NH cross-peaks for residues Arg1, Arg9, Arg10, and Arg18 were completely broadened, possibly, due to the chemical exchange of the amide protons with solvent. In the homology model of **13** (**Fig. 6B**), which is based on the wt RTD-1, the amides of Arg1, Arg9, Arg10, and Arg18 are located in the loops and are solvent exposed; these two conditions facilitate amide-solvent proton chemical exchange.

Based on the assigned cysteine Cβ chemical shifts (**Table S2**), all cysteine residues in peptide **13** form disulfide bonds. Although clearly visible, the corresponding Cys NH cross-peaks were broadened in the nitrogen dimension when compared to those from the Trp or Arg residues. Broadening of the Cys NH cross-peaks has been attributed to the isomerization of disulfide bonds in other Cys-rich polypeptides.[36, 37] Cys amides were clustered in two distinct groups, suggesting two different types of similar chemical environments. Interestingly the backbone cross-peaks for the Cys residues C5 and C14 were identical indicating the presence of a symmetry element between these two residues.

Backbone, HN, Hα, N, Cα, and side chain Cβ chemical shifts are exquisitely sensitive to the protein conformation and used to establish secondary structure fold. We used the chemical shift index (CSI),[38] which is calculated based on the difference between protein chemical shifts and that of random coil, to identify the secondary structure elements within the sequence of p□□□□□□□□**13**. The CSI values per residue of peptide **7** were consistent with segments Phe2-Arg8

and Val11-Thr17 adopting an antiparallel β-sheet structure, and with residues Arg1, Arg9, Arg10, and Arg18 located in the corresponding connecting loops (**Figs. S11** and **S12**). In addition, we were able to identify seventeen interresidual NOEs for peptide **13** (**Table S3**). The number of unambiguous NOEs was much lower that what is required for the determination of a high-resolution structure, usually 5 NOEs/residue. This was due to the highly symmetrical nature of peptide **13** primary structure, which resulted in the extremely overlapped NMR spectra. Nevertheless, these experimental data, altogether, are fully consistent with peptide **13** adopting a native θ-defensin fold.

DISCUSSION AND CONCLUSIONS

We report the first full sequence amino acid scanning of backbone-cyclized θ-defensin to improve its biological activity against the anthrax metalloprotease LF. LF protease is a component of the lethal factor toxin produced by the bacterium *Bacillus anthracis*, which is key to the pathogenesis of anthrax,[24] and therefore a therapeutic target for the development of novel potential treatments for anthrax disease.[25] The LF catalyzes the hydrolysis of mitogen-activated protein kinase kinase 1 (MAPKK1) and MAPKK2 rendering them inactive and hence incapable of activating the mitogen-activated protein protein kinase (MAPK) pathway.[39, 40] Cleavage of the MAPKK proteins leads to inhibition of a wide variety of immune cell functions, cellular necrosis and apoptosis.[24]

Wild-type RTD-1 is a moderate non-competitive inhibitor of LF protease (K_i = 365 ± 20 nM) and a weak inhibitor of other metalloproteases such as TACE (K_i = 4.45 ± 0.48 μM). We have used a full sequence amino acid scanning approach to explore the contribution of every amino acid, except the Cys residues required for folding, to the anti-LF activity and whether this could be improved by replacing the original residue with a set of different amino acids including hydrophobic,

aromatic, positively and negatively charged residues. This required the synthesis of over 100 individual θ-defensin analogs. Defensin analogs were rapidly produced in high purity by using a novel approach for the rapid parallel production of disulfide-rich backbone cyclized polypeptides using a 'tea-bag' approach in combination with high efficient cyclization-folding protocols that require minimal purification.[22, 23]

In general, all the positions in RTD-1 were amenable to mutation with exception of the Arg residues (Arg4 and Arg13) located in the β-sheet region of the peptide. In our hands, replacement of these residues by non-charged residues yielded cyclic peptides that could not fold correctly. Regarding the biological activity of RTD-1, the presence of a θ-defensin fold is required for biological activity. Replacement of the Cys residues by Ser yielded an inactive peptide against LF (IC_{50} >10 μM). Also, we found that the native Arg residues in RTD-1 are key for anti-LF activity. Replacement of these residues by negatively charged amino acids, Asp or Glu, decreased the biological activity of the resulting peptides. In addition, introduction of extra Arg residues in the non-hydrophobic residues located in both loops (Gly1, Gly10 and Thr17) also gave peptides with improved biological activity. Replacement of the hydrophobic residues in RTD-1 by Trp was also able to increase the anti-LF activity. Using this information, we were able to design a series of RTD-1 analogs with increasing activities for inhibiting LF. The most active compound, peptide **13**, was about 10 times more active than native RTD-1, IC_{50} value of 43 ± 3 nM *versus* 390 ± 20 nM for RTD-1. P□□□□□□ **7** was able to fold adopting a native θ-defensin fold as determined by NMR, despite the numerous mutations introduced in this peptide. Intriguingly, peptide **13** has a symmetrical sequence almost entirely composed by Arg and Trp residues, with the exception of the Cys residues that are required for disulfide formation and folding. Despite the high content on Arg and Trp residues, θ-defensin **13** was not cytotoxic to mammalian cells up to a concentration of 100 μM. This peptide was able to retain significant

anti-LF activity even in the presence of bovine serum albumin, while was not active under the same conditions against the metalloprotease TACE (IC_{50} > 10 μM). The TACE inhibitory activity of different RTD-1 analogs was also analyzed indicating a different mechanism of inhibition in both proteases. For example, introduction of negative charge in RTD-1 was able to improve the anti-TACE activity while had a negative effect on the anti-LF activity (**Table 1**). More intriguing was the result obtained with the V11W mutant (peptide **7**), which increased the TACE inhibitory activity over 25 times while the same mutant had only a modest effect on anti-LF activity (**Table 1**). All combined, these data suggest that peptide **13** does not inhibit LF through a non-specific mechanism, although more structural studies may be required to fully understand at the molecular level the mechanism of inhibition of this peptide.

A recent study has reported that retrocyclins, synthetic peptides corresponding to a putative ancestral human peptide encoded by a θ-defensin pseudogene,[13] are able to destabilize some bacterial toxins causing them to unfold in thermal denaturation assays.[41] Precipitation of bacterial toxins in the presence of defensins has been also described as a mechanism the inactivation of some bacterial toxins by these types of peptides.[42] In our study, however, we did not see any evidence of protein precipitation under the conditions used in our assays.

In summary, we report the use of amino acid positional scanning to improve the inhibitory activity of the θ-defensin RTD-1 against the bacterial metalloprotease LF. Our results clearly show the high robustness of the θ-defensin scaffold for the generation of molecular diversity, either generated by chemical synthesis (this work) or recombinant expression methods.[43] These libraries should allow the rapid screening and selection of novel θ-defensin-based sequences able to inhibit other proteases or modulate specific protein/protein interactions, therefore providing leads for the development of novel peptide-based therapeutics.

EXPERIMENTAL SECTION

Analytical HPLC was performed on a HP1100 series instrument with 220 nm and 280 nm detection using a Vydac C18 column (5 mm, 4.6 x 150 mm) at a flow rate of 1 mL/min. All runs used linear gradients of 0.1% aqueous trifluoroacetic acid (TFA, solvent A) vs. 0.1% TFA, 90% acetonitrile in H_2O (solvent B). UV-vis spectroscopy was carried out on an Agilent 8453 diode array spectrophotometer, and fluorescence analysis on a Jobin Yvon Flurolog-3 spectroflurometer. Electrospray mass spectrometry (ES-MS) analysis was performed on an Applied Biosystems API 3000 triple quadrupole electrospray mass spectrometer using software Analyst 1.4.2. Calculated masses were obtained using Analyst 1.4.2. All chemicals involved in synthesis or analysis were obtained from Aldrich (Milwaukee, WI) or Novabiochem (San Diego, CA) unless otherwise indicated. The purity of all the peptides used in this study was estimated to be ≥95% as determined by HPLC and ES-MS.

Preparation of Fmoc-Aaa-OH. Fmoc-Phe-F and Fmoc-Leu-F were prepared using diethylaminosulfur trifluoride (DAST) as previously described[23] and quickly used afterwards. Briefly, DAST (160 μL, 1.2 mmol) was added drop wise at 25° C under nitrogen current to a stirred solution of Fmoc-Phe-OH (387.4 mg, 1 mmol) or Fmoc-Leu-OH (353.4 mg, 1 mmol) in 10 mL of dry dichloromethane (DCM), containing dry pyridine (81 μL, 1 mmol). After 20 minutes, the mixture was washed with ice-cold water (3 x 20 mL). The organic layer was separated and dried over anhydrous $MgSO_4$. The solvent was removed under reduced pressure to give the corresponding Fmoc-amino acyl fluoride as white solid that was immediately used.

Loading of 4-sulfamylbutyryl AM resin with Fmoc-Aaa-F. Loading of the first residue was accomplished using Fmoc-Phe-F or Fmoc-Leu-F as previously described.[23]. Briefly, 4-

sulfamylbutyryl AM resin (420 mg, 0.33 mmol) (Novabiochem) was swollen for 20 minutes with dry DCM and then drained. A solution of Fmoc-Phe-F (≈389 mg, ≈1 mmol) of Fmoc-Leu-OH (≈354 mg, ≈ 1 mmol) in dry DCM (2 mL) and di-isopropylethylamine (DIEA) (180 µL, 1 mmol) was added to the drained resin and reacted at 25° C for 1 h. The resin was washed with dry DCM (5 x 5 mL), dried and kept at -20° C until use.

Chemical synthesis of RTD-1 based peptides. All peptides were synthesized as described in **Fig. 2** and was carried out by solid-phase synthesis on an automatic peptide synthesizer ABI433A (Applied Biosystems) using the Fast-Fmoc chemistry with 2-(1H-benzotriazol-1-yl)-1,1,3,3-tetramethyluronium hexafluorophosphate (HBTU)/diisopropylethylamine (DIEA) activation protocol at 0.1 mmol scale on a Fmoc-Phe-sulfamylbutyryl AM resin (L6 and R4 position scanning library) or Fmoc-Leu-sulfamylbutyryl AM resin (the rest of peptides). Side-chain protection compatible with Fmoc-chemistry was employed as previously described for the synthesis of peptide α-thioesters by the Fmoc-protocol, except for the N-terminal Cys residue, which was introduced as Boc-Cys(Trt)-OH. Before coupling of the position to be scanned, the peptide-resin was manually resuspended in DCM:dimethylformamide (DMF)(1:1) and split into 9 equal aliquots. Each peptide-resin aliquot was placed in a separate 1 mL polypropylene column (Qiagen). The resins were manually deprotected with 20% 4-methylpiperidine in DMF (3 x 5 min) and then individually coupled with each of the different 9 Fmoc-Aaa-OH (**Figs. 1** and **2**). Couplings were performed using HBTU and DIEA for 45 min. The resins were then washed, dried, placed in individual tagged 'tea-bags' (30 x 20 mm) and sealed. The synthesis was continued using the peptide synthesizer 0.25 mmol reaction vessel, which can hold up to 9 different tea-bags of the dimensions reported above. Following chain assembly, the alkylation, thiolytic cleavage and side chain deprotection were performed for individual peptides in 1 mL polypropylene columns as previously described.[44] Briefly, ≈10 mg of protected peptide-resin

were first alkylated two times with ICH_2CN (17.4 µL, 0.24 mmol; previously filtered through basic alumina) and DIEA (8.2 µL, 0.046 mmol) in N-methylpyrrolidone (NMP) (0.22 mL) for 24 h. The resin was then washed with NMP (3 x 5 mL) and DCM (3 x 5 mL). The alkylated peptide resin was cleaved from the resin with $HSCH_2CH_2CO_2Et$ (20 µL, 0.18 mmol) in the presence of a catalytic amount of sodium thiophenolate (NaSPh, 0.3 mg, 2.2 µmol) in DMF:DCM (1:2 v/v, 0.12 mL) for 24 h. The resin was then dried at reduced pressure. The side-chain protecting groups were removed by treating the dried resin with trifluoroacetic acid (TFA):H_2O:tri-isopropylsilane (TIS) (95:3:2 v/v, 0.5 mL) for 3-4 h at room temperature. The resin was filtered and the linear peptide thioester was precipitated in cold Et_2O. The crude material was dissolved in the minimal amount of H_2O:MeCN (4:1) containing 0.1% TFA and characterized by HPLC and ES-MS as the corresponding desired linear precursor α-thioester. Cyclization and folding was accomplished by flash dilution of the linear α-thioester TFA crude to a final concentration of ≈20-50 µM into freshly degassed 2 mM reduced glutathione (GSH), 0.1 M sodium phosphate buffer at pH 7.2 for 96 h. Most RTD-1 analogs were desalted using a C18 cartridge solid phase extraction (SPE) to remove the buffer components providing the folded peptide with relatively high purity (**Fig. S1**). Single mutants R8L and V11E, and peptides **8** through **13** were purified by C18-reversed-phase HPLC and characterized by ES-MS (**Fig. S3 and S5**). The complete synthesis of a positional sub-library took around 1.5 weeks in average, from the start of the synthesis to the lyophilized purified peptide.

Synthesis of peptide 1. The linear thioester precursor of peptide control **1** was synthesized as described above. Cyclization was accomplished by flash dilution of the linear α-thioester to a final concentration of 25 µM into freshly degassed 2% sodium 2-mercaptoethanesulfonate (MESNA) in 0.1 M sodium phosphate buffer at pH 7.2 for 1 h. S-alkylation was achieved by adding a large excess of iodoacetamide into the cyclization mixture for 30 min. The final peptide

was purified using a linear gradient 15-25% buffer B over 30 min and characterized by analytical HPLC and ES-MS (**Fig. S8**).

Peptide quantification. RTD-1 peptide analogs were quantified by HPLC at 214 nm using a relative extinction coefficient calculated as previously described.[45] A solution of pure peptide RTD-1 of known concentration estimated by amino acid analysis was used as internal control for HPLC quantification.

Anthrax LF protease inhibition assay. Lethal factor (LF) protease and FRET-based substrate containing fluorescent proteins CyPet and YPet linked by consensus sequence (RRKKVYPYPMEGTIA) containing the linker $(GGS)_6$ at both sites of the consensus sequence were expressed and purified as previously described.[29, 46] LF inhibition assay was performed in LF reaction buffer (10 μM $CaCl_2$, 10 μM $MgCl_2$, 20 μM $ZnCl_2$, 20 mM sodium phosphate, and 100 mM NaCl at pH 7.2) in the presence or absence of BSA. Samples of 50 nM LF in LF reaction buffer (100 μL) were preincubated with different concentrations of RTD-1 ranging from 1 nM to 10 μM. After incubation at room temperature for 30 min, residual LF activity was measured by adding the FRET-based substrate to a final concentration of 10 nM and the decrease in FRET signal was measured every 2 min for 3 h.[29] FRET was measured using an Envision 2103 plate reader (PerkinElmer) using an excitation wavelength of 405 nm. The relative FRET change was calculated using: FRC = I_t^{535}/I_0^{535}, where I_0 and I_t are the fluorescence intensities at time zero and at a particular time (t), at 535 nm. The initial velocities for the hydrolysis of substrate Lethal Factor in the presence of different concentrations of RTD-1 were fitted to a log(inhibitor) *versus* response with a variable Hill-slope using the software package Prism (GraphPad Software). K_i was calculated using the equation for non-competitive tightly bound inhibitors; where $K_i = IC_{50} - E_0/2$ (E_0 = enzyme concentration).[47, 48]

TACE protease inhibition assay. TACE protease containing the catalytic domain (TACE (233-477), Enzo Life Sciences) or the whole extracellular domain (TACE (215-671), R&D System), and the TACE fluorogenic substrate (Mca-Pro-Leu-Ala-Gln-Ala-Val-Dpa-Arg-Ser-Ser-Ser-Arg-NH_2, Enzo Life Sciences, where Mca = (7-methoxycoumarin-4-yl)acetyl and Dpa = N-3-(2,4-dinitrophenyl)-L-α,β-diaminopropionyl) were used in this work. The proteolytic reaction was performed in TACE reaction buffer (2.5 μM $ZnCl_2$ and 25 mM Tris-HCl, at pH 8.0) in the presence or absence of BSA. Samples of 2 nM TACE in TACE reaction buffer (100 μL) were preincubated with different concentrations of RTD-1 based peptides ranging from 1 nM to 10 μM. After incubation at room temperature for 30 min, residual TACE activity was measured by adding the fluorogenic substrate to a final concentration of 3 μM. Fluorescence was measured every 2 min for 3 h in an Envision 2103 plate reader (PerkinElmer) using an excitation wavelength of 320 nm and an emission wavelength of 405 nm. The initial velocities for the increase of fluorescent signal in the presence of different concentrations of the corresponding RTD-1 analog were calculated as described earlier for LF. The K_i values were calculated as for LF.

Bacterial expression of ^{15}N-labeled of θ-defensin 13. Bacterial expression of ^{15}N- and ^{13}C,^{15}N-labeled **13** was achieved as previously described.[43] The purified peptides were characterized by analytical HPLC and ES-MS (**Fig. S9**).

Cytotoxicity Assay

HeLa cells were cultured in DMEM medium supplemented with 10% fetal bovine serum (FBS), penicillin (50 IU/mL), and streptomycin (50 μg/mL) at 37° C with 5% CO_2. The cellular toxicity of the RTD-1 peptides was measured using an MTT assay as previously described.[49] Briefly, ≈3 x 10^3 cells were seeded in 96-well microtiter plates in 100 μL DMEM with 10% FBS and incubated for 24 h. After the incubation period, the cells were washed with PBS and treated with 200 μL/well DMEM media supplemented with 10% FBS containing the peptides at the indicated

concentration for 48 h at 37° C in 5% CO_2 and then treated with 20 µL of a solution of 3-(4,5-dimethylthiazol-2-yl)-2,5-diphenyltetrazolium bromide (MTT, 5 mg/mL) for 2 h. The medium was discarded and DMSO (100 µL/well) was added to each well and incubated with gentle shaking for 20 min at room temperature. The absorbance at 595 nm of the solution was analyzed using a Tecan Genios Multifunctional Microplate Reader (Tecan System Inc) and the background at 670 nm subtracted.

Molecular modeling and dynamics of θ-defensin 13. The homology model of θ-defensin **13** was built using the structure of RTD-1 (PDB ID code: 1HVZ)[6] as template. The resulting structure was subjected to molecular dynamics for 700 ns in a neutral water box containing 0.9% NaCl. The molecular dynamics was run using the macro md_run.mcr (www.yasara.org/md_run.mcr) using the Yasara software package (www.yasara.org). The 10 most stable structures were used to generate a morphed movie using Pymol (www.pymol.org) (**Fig. S14**).

NMR spectroscopy. NMR samples were prepared by dissolving **13** into 80 mM potassium phosphate pH 6.5, 0.05% trifluoracetic acid, 100 mM d6-DMSO in 90% H_2O/10% ^2H_2O (v/v) to a concentration of approximately 0.2 mM for unlabeled **13** and 0.1 mM for [*U*- ^{15}N] and [*U*- ^{13}C, ^{15}N] peptide **13**. All NMR spectra were acquired on a Bruker Avance III 600 MHz spectrometer equipped with TCI cryoprobe. The NMR spectra were acquired at 298 K, and 2,2-dimethyl-2-silapentane-5-sulfonate, DSS, was used as an internal reference. The carrier frequency was centered on the water signal, and the solvent was suppressed by using either WATERGATE pulse sequence or a spin lock pulse. Standard triple resonance experiments HNCACB and CBCACONH as well as HCCH-TOCSY, 3D ^{1}H, ^{15}N-NOESY (mixing time 200 ms), 2D ^{13}C-HSQC, ^{15}N-HSQC, ^{1}H, ^{1}H-NOESY (mixing time 200 ms), 3D ^{1}H, ^{15}N-TOCSY (spin lock time 80 ms), and 2D ^{1}H, ^{1}H-TOCSY (spin lock time 80 ms) were collected.[50] Spectra were processed using Topspin 3.1 (Bruker).

Assignments for the backbone nitrogen (^{15}N), carbons (Cα and Cβ) and protons (Hα and NH) of peptide **13** (**Table S2**) were obtained using standard procedures.[51, 52]

Supporting Information Available: Analytical, biological and NMR data on the θ-defensin peptide analogs produced in this work. The coordinates for the homology model of θ-defensin **13** are also included. This material is available free of charge via the Internet at http://pubs.acs.org.

Homology Models: The coordinates for the homology model of θ-defensin **13** are included in the Supporting Information.

Corresponding Author Information: Julio A. Camarero, Ph.D., Department of Pharmacology and Pharmaceutical Sciences, Department of Chemistry, University of Southern California, 1985 Zonal Avenue, PSC 616, Los Angeles, CA 90033, Tel: 323-442-1417, Fax: 323-224-7473, E-mail: jcamarer@usc.edu.

Abbreviations used: ES-MS, electrospray mass spectrometry; GSH, glutathione; LF, lethal factor; RTD-1, Rhesus θ-defensin; TACE: TNFα converting enzyme

Acknowledgements: We thank Drs. Michael E. Selsted and Andre J. Ouellette (University of Southern California) for their suggestions and help during this project. This work was supported by National Institutes of Health Research Grants R01-GM090323 (J.A.C.), R01-GM113363 (J.A.C.) and R01-GM085006 (A.S.).

References

1. Tang, Y. Q.; Yuan, J.; Osapay, G.; Osapay, K.; Tran, D.; Miller, C. J.; Ouellette, A. J.; Selsted, M. E. A cyclic antimicrobial peptide produced in primate leukocytes by the ligation of two truncated alpha-defensins. *Science* **1999,** *286*, 498-502.

2. Tanabe, H.; Yuan, J.; Zaragoza, M. M.; Dandekar, S.; Henschen-Edman, A.; Selsted, M. E.; Ouellette, A. J. Paneth cell alpha-defensins from rhesus macaque small intestine. *Infect. Immun.* **2004,** *72*, 1470-1478.

3. Selsted, M. E.; Ouellette, A. J. Mammalian defensins in the antimicrobial immune response. *Nat. Immunol.* **2005,** *6*, 551-557.

4. Lehrer, R. I. Primate defensins. *Nat. Rev. Microbiol.* **2004,** *2*, 727-738.

5. Rosengren, K. J.; Daly, N. L.; Fornander, L. M.; Jonsson, L. M.; Shirafuji, Y.; Qu, X.; Vogel, H. J.; Ouellette, A. J.; Craik, D. J. Structural and functional characterization of the conserved salt bridge in mammalian paneth cell alpha-defensins: solution structures of mouse CRYPTDIN-4 and (E15D)-CRYPTDIN-4. *J. Biol. Chem.* **2006,** *281*, 28068-28078.

6. Trabi, M.; Schirra, H. J.; Craik, D. J. Three-dimensional structure of RTD-1, a cyclic antimicrobial defensin from Rhesus macaque leukocytes. *Biochemistry* **2001,** *40*, 4211-4221.

7. Leonova, L.; Kokryakov, V. N.; Aleshina, G.; Hong, T.; Nguyen, T.; Zhao, C.; Waring, A. J.; Lehrer, R. I. Circular minidefensins and posttranslational generation of molecular diversity. *J. Leukoc. Biol.* **2001,** *70*, 461-464.

8. Tran, D.; Tran, P. A.; Tang, Y. Q.; Yuan, J.; Cole, T.; Selsted, M. E. Homodimeric theta-defensins from rhesus macaque leukocytes: isolation, synthesis, antimicrobial activities, and bacterial binding properties of the cyclic peptides. *J. Biol. Chem.* **2002,** *277*, 3079-3084.

9. Tongaonkar, P.; Tran, P.; Roberts, K.; Schaal, J.; Osapay, G.; Tran, D.; Ouellette, A. J.; Selsted, M. E. Rhesus macaque theta-defensin isoforms: expression, antimicrobial activities, and demonstration of a prominent role in neutrophil granule microbicidal activities. *J. Leukoc. Biol.* **2011,** *89*, 283-290.

10. Nguyen, T. X.; Cole, A. M.; Lehrer, R. I. Evolution of primate theta-defensins: a serpentine path to a sweet tooth. *Peptides* **2003,** *24*, 1647-1654.

11. Garcia, A. E.; Osapay, G.; Tran, P. A.; Yuan, J.; Selsted, M. E. Isolation, synthesis, and antimicrobial activities of naturally occurring theta-defensin isoforms from baboon leukocytes. *Infect. Immun.* **2008,** *76*, 5883-5891.

12. Stegemann, C.; Tsvetkova, E. V.; Aleshina, G. M.; Lehrer, R. I.; Kokryakov, V. N.; Hoffmann, R. De novo sequencing of two new cyclic theta-defensins from baboon (Papio hamadryas) leukocytes by matrix-assisted laser desorption/ionization mass spectrometry. *Rapid. Commun. Mass Spectrom.* **2010,** *24*, 599-604.

13. Cole, A. M.; Hong, T.; Boo, L. M.; Nguyen, T.; Zhao, C.; Bristol, G.; Zack, J. A.; Waring, A. J.; Yang, O. O.; Lehrer, R. I. Retrocyclin: a primate peptide that protects cells from infection by T- and M-tropic strains of HIV-1. *Proc. Natl. Acad. Sci. U.S.A.* **2002,** *99*, 1813-1818.

14. Tran, D.; Tran, P.; Roberts, K.; Osapay, G.; Schaal, J.; Ouellette, A.; Selsted, M. E. Microbicidal properties and cytocidal selectivity of rhesus macaque theta defensins. *Antimicrob. Agents Chemother.* **2008,** *52*, 944-953.

15. Penberthy, W. T.; Chari, S.; Cole, A. L.; Cole, A. M. Retrocyclins and their activity against HIV-1. *Cell. Mol. Life. Sci.* **2011,** *68*, 2231-2242.

16. Munk, C.; Wei, G.; Yang, O. O.; Waring, A. J.; Wang, W.; Hong, T.; Lehrer, R. I.; Landau, N. R.; Cole, A. M. The theta-defensin, retrocyclin, inhibits HIV-1 entry. *AIDS Res. Hum. Retroviruses* **2003,** *19*, 875-881.

17. Owen, S. M.; Rudolph, D.; Wang, W.; Cole, A. M.; Sherman, M. A.; Waring, A. J.; Lehrer, R. I.; Lal, R. B. A theta-defensin composed exclusively of D-amino acids is active against HIV-1. *J. Pept. Res.* **2004,** *63*, 469-476.

18. Gallo, S. A.; Wang, W.; Rawat, S. S.; Jung, G.; Waring, A. J.; Cole, A. M.; Lu, H.; Yan, X.; Daly, N. L.; Craik, D. J.; Jiang, S.; Lehrer, R. I.; Blumenthal, R. Theta-defensins prevent HIV-1 Env-mediated fusion by binding gp41 and blocking 6-helix bundle formation. *J. Biol. Chem.* **2006,** *281*, 18787-18792.

19. Wang, W.; Mulakala, C.; Ward, S. C.; Jung, G.; Luong, H.; Pham, D.; Waring, A. J.; Kaznessis, Y.; Lu, W.; Bradley, K. A.; Lehrer, R. I. Retrocyclins kill bacilli and germinating spores of Bacillus anthracis and inactivate anthrax lethal toxin. *J. Biol. Chem.* **2006,** *281*, 32755-32764.

20. Schaal, J. B.; Tran, D.; Tran, P.; Osapay, G.; Trinh, K.; Roberts, K. D.; Brasky, K. M.; Tongaonkar, P.; Ouellette, A. J.; Selsted, M. E. Rhesus macaque theta defensins suppress inflammatory cytokines and enhance survival in mouse models of bacteremic sepsis. *PLoS One* **2012,** *7*, e51337.

21. Tongaonkar, P.; Trinh, K. K.; Schaal, J. B.; Tran, D.; Gulko, P. S.; Ouellette, A. J.; Selsted, M. E. Rhesus macaque theta-defensin RTD-1 inhibits proinflammatory cytokine secretion and gene expression by inhibiting the activation of NF-kappaB and MAPK pathways. *J. Leukoc. Biol.* **2015,** *98*, 1061-1070.

22. Aboye, T. L.; Li, Y.; Majumder, S.; Hao, J.; Shekhtman, A.; Camarero, J. A. Efficient one-pot cyclization/folding of rhesus theta-defensin-1 (RTD-1). *Bioorg. Med. Chem. Lett.* **2012,** *22*, 2823-2826.

23. Aboye, T.; Kuang, Y.; Neamati, N.; Camarero, J. A. Rapid parallel synthesis of bioactive folded cyclotides by using a tea-bag approach. *Chembiochem* **2015,** *16*, 827-833.

24. Moayeri, M.; Leppla, S. H. Cellular and systemic effects of anthrax lethal toxin and edema toxin. *Mol. Aspects Med.* **2009,** *30*, 439-455.

25. Moayeri, M.; Crown, D.; Jiao, G. S.; Kim, S.; Johnson, A.; Leysath, C.; Leppla, S. H. Small-molecule inhibitors of lethal factor protease activity protect against anthrax infection. *Antimicrob. Agents Chemother.* **2013,** *57*, 4139-4145.

26. Backes, B. J.; Ellman, J. A. An alkanesulfonamide "safety-catch" linker for solid-phase synthesis. *J. Org. Chem.* **1999,** *64*, 2322-2330.

27. Shin, Y.; Winans, K. A.; Backes, B. J.; Kent, S. B. H.; Ellman, J. A.; Bertozzi, C. R. Fmoc-Based synthesis of peptide-$^{\alpha}$thioesters: Application to the total chemical synthesis of a glycoprotein by native chemical ligation. *J. Am. Chem. Soc.* **1999,** *121*, 11684-11689.

28. Ingenito, R.; Bianchi, E.; Fattori, D.; Pessi, A. Solid phase synthesis of peptide C-terminal thioesters by Fmoc/t-Bu chemistry. *J. Am. Chem. Soc.* **1999,** *121*, 11369-11374.

29. Kimura, R. H.; Steenblock, E. R.; Camarero, J. A. Development of a cell-based fluorescence resonance energy transfer reporter for Bacillus anthracis lethal factor protease. *Anal. Biochem.* **2007,** *369*, 60-70.

30. Black, R. A.; Rauch, C. T.; Kozlosky, C. J.; Peschon, J. J.; Slack, J. L.; Wolfson, M. F.; Castner, B. J.; Stocking, K. L.; Reddy, P.; Srinivasan, S.; Nelson, N.; Boiani, N.; Schooley, K. A.; Gerhart, M.; Davis, R.; Fitzner, J. N.; Johnson, R. S.; Paxton, R. J.; March, C. J.; Cerretti, D. P. A metalloproteinase disintegrin that releases tumour-necrosis factor-alpha from cells. *Nature* **1997,** *385*, 729-733.

31. Moss, M. L.; Jin, S. L.; Milla, M. E.; Burkhart, W.; Carter, H. L.; Chen, W. J.; Clay, W. C.; Didsbury, J. R.; Hassler, D.; Hoffman, C. R.; Kost, T. A.; Lambert, M. H.; Leesnitzer, M. A.; McCauley, P.; McGeehan, G.; Mitchell, J.; Moyer, M.; Pahel, G.; Rocque, W.; Overton, L. K.; Schoenen, F.; Seaton, T.; Su, J. L.; Warner, J; Willard, D.; Becherer, J. D. Cloning of a disintegrin metalloproteinase that processes precursor tumour-necrosis factor-alpha. *Nature* **1997,** *385*, 733-736.

32. Moss, M. L.; Sklair-Tavron, L.; Nudelman, R. Drug insight: tumor necrosis factor-converting enzyme as a pharmaceutical target for rheumatoid arthritis. *Nat. Clin. Pract. Rheumatol.* **2008,** *4*, 300-309.

33. Rose-John, S. ADAM17, shedding, TACE as therapeutic targets. *Pharmacol. Res.* **2013,** *71*, 19-22.

34. Pereira, M. P.; Blanchard, J. E.; Murphy, C.; Roderick, S. L.; Brown, E. D. High-throughput screening identifies novel inhibitors of the acetyltransferase activity of Escherichia coli GlmU. *Antimicrob. Agents Chemother.* **2009,** *53*, 2306-2311.

35. Haque, A.; Tonks, N. K. The use of phage display to generate conformation-sensor recombinant antibodies. *Nat. Protoc.* **2012,** *7*, 2127-2143.

36. Grey, M. J.; Wang, C.; Palmer, A. G., 3rd. Disulfide bond isomerization in basic pancreatic trypsin inhibitor: multisite chemical exchange quantified by CPMG relaxation dispersion and chemical shift modeling. *J. Am. Chem. Soc.* **2003,** *125*, 14324-14335.

37. Puttamadappa, S. S.; Jagadish, K.; Shekhtman, A.; Camarero, J. A. Backbone dynamics of cyclotide MCoTI-I free and complexed with trypsin. *Angew. Chem. Int. Ed. Engl.* **2010,** *49*, 7030-7034.

38. Hafsa, N. E.; Arndt, D.; Wishart, D. S. CSI 3.0: a web server for identifying secondary and super-secondary structure in proteins using NMR chemical shifts. *Nucleic Acids Res.* **2015,** *43*, W370-377.

39. Vitale, G.; Bernardi, L.; Napolitani, G.; Mock, M.; Montecucco, C. Susceptibility of mitogen-activated protein kinase kinase family members to proteolysis by anthrax lethal factor. *Biochem. J.* **2000,** *352*, 739-745.

40. Duesbery, N. S.; Webb, C. P.; Leppla, S. H.; Gordon, V. M.; Klimpel, K. R.; Copeland, T. D.; Ahn, N. G.; Oskarsson, M. K.; Fukasawa, K.; Paull, K. D.; Vande Woude, G. F. Proteolytic inactivation of MAP-kinase-kinase by anthrax lethal factor. *Science* **1998,** *280*, 734-737.

41. Kudryashova, E.; Seveau, S.; Lu, W.; Kudryashov, D. S. Retrocyclins neutralize bacterial toxins by potentiating their unfolding. *Biochem. J.* **2015,** *467*, 311-320.

42. Lehrer, R. I.; Jung, G.; Ruchala, P.; Wang, W.; Micewicz, E. D.; Waring, A. J.; Gillespie, E. J.; Bradley, K. A.; Ratner, A. J.; Rest, R. F.; Lu, W. Human alpha-defensins inhibit hemolysis mediated by cholesterol-dependent cytolysins. *Infect. Immun.* **2009,** *77*, 4028-4040.

43. Gould, A.; Li, Y.; Majumder, S.; Garcia, A. E.; Carlsson, P.; Shekhtman, A.; Camarero, J. A. Recombinant production of rhesus theta-defensin-1 (RTD-1) using a bacterial expression system. *Mol. Biosyst.* **2012,** *8*, 1359-1365.

44. Contreras, J.; Elnagar, A. Y.; Hamm-Alvarez, S. F.; Camarero, J. A. Cellular uptake of cyclotide MCoTI-I follows multiple endocytic pathways. *J. Control Release* **2011,** *155*, 134-143.

45. Kuipers, B. J.; Gruppen, H. Prediction of molar extinction coefficients of proteins and peptides using UV absorption of the constituent amino acids at 214 nm to enable quantitative reverse phase high-performance liquid chromatography-mass spectrometry analysis. *J. Agric. Food Chem.* **2007,** *55*, 5445-5451.

46. Kwon, Y.; Welsh, K.; Mitchell, A. R.; Camarero, J. A. Preparation of peptide p-nitroanilides using an aryl hydrazine resin. *Org. Lett.* **2004,** *6*, 3801-3804.

47. Cer, R. Z.; Mudunuri, U.; Stephens, R.; Lebeda, F. J. IC50-to-Ki: a web-based tool for converting IC50 to Ki values for inhibitors of enzyme activity and ligand binding. *Nucleic Acids Res.* **2009,** *37*, W441-445.

48. Cha, S. Tight-binding inhibitors-I. Kinetic behavior. *Biochem. Pharmacol.* **1975,** *24*, 2177-2185.

49. Ji, Y.; Majumder, S.; Millard, M.; Borra, R.; Bi, T.; Elnagar, A. Y.; Neamati, N.; Shekhtman, A.; Camarero, J. A. In vivo activation of the p53 tumor suppressor pathway by an engineered cyclotide. *J. Am. Chem. Soc.* **2013,** *135*, 11623-11633.

50. Cavanagh, J.; Fairbrother, W. J.; Palmer, A. G.; Rance, M.; Skelton, N. J. P*rotein NMR spectroscopy: principles and practice*, 2nd ed.; Elsevier Inc., 2007.

51. Cavanagh, J.; Rance, M. Suppression of cross relaxation effects in TOCSY spectra via a modified DISI-2 mixing sequence. *J. Magn. Res.* **1992,** 96, 670-678.

52. Wuthrich, K. *NMR of proteins and nucleic Acids*; Wiley, 1986.

Figures and Tables

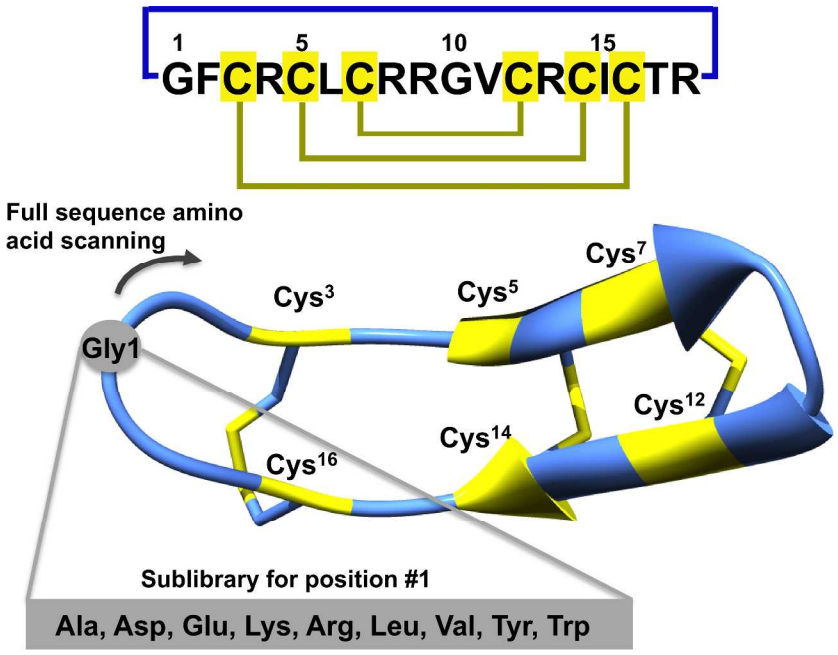

Figure 1. Primary and tertiary structure of rhesus θ-defensin 1 (RTD-1) (PDB ID code: 1HVZ).[6] The backbone cyclized peptide (connecting bond shown in blue) is stabilized by the three disulfide bonds in a ladder formation (disulfide bonds shown in yellow). Scheme showing the amino acid scanning approach used in this work. Residues in RTD-1, except for the Cys residues, were replaced by a set of amino acids containing Ala, Asp, Glu, Leu, Val, Lys, Arg, Tyr or Trp. When the native the residue on the RTD-1 sequence was Arg, Leu, or Val, the corresponding amino in the set indicated above was replaced by His (Arg) or Ile (Val and Leu). Also, Leu was not included in the Phe2 sub-library therefore containing only 8 members. Accordingly, a total of 107 (=11 x 9 + 1 x 8) different f RTD-1 variants containing a single mutation were chemically prepared (**Table S1**).

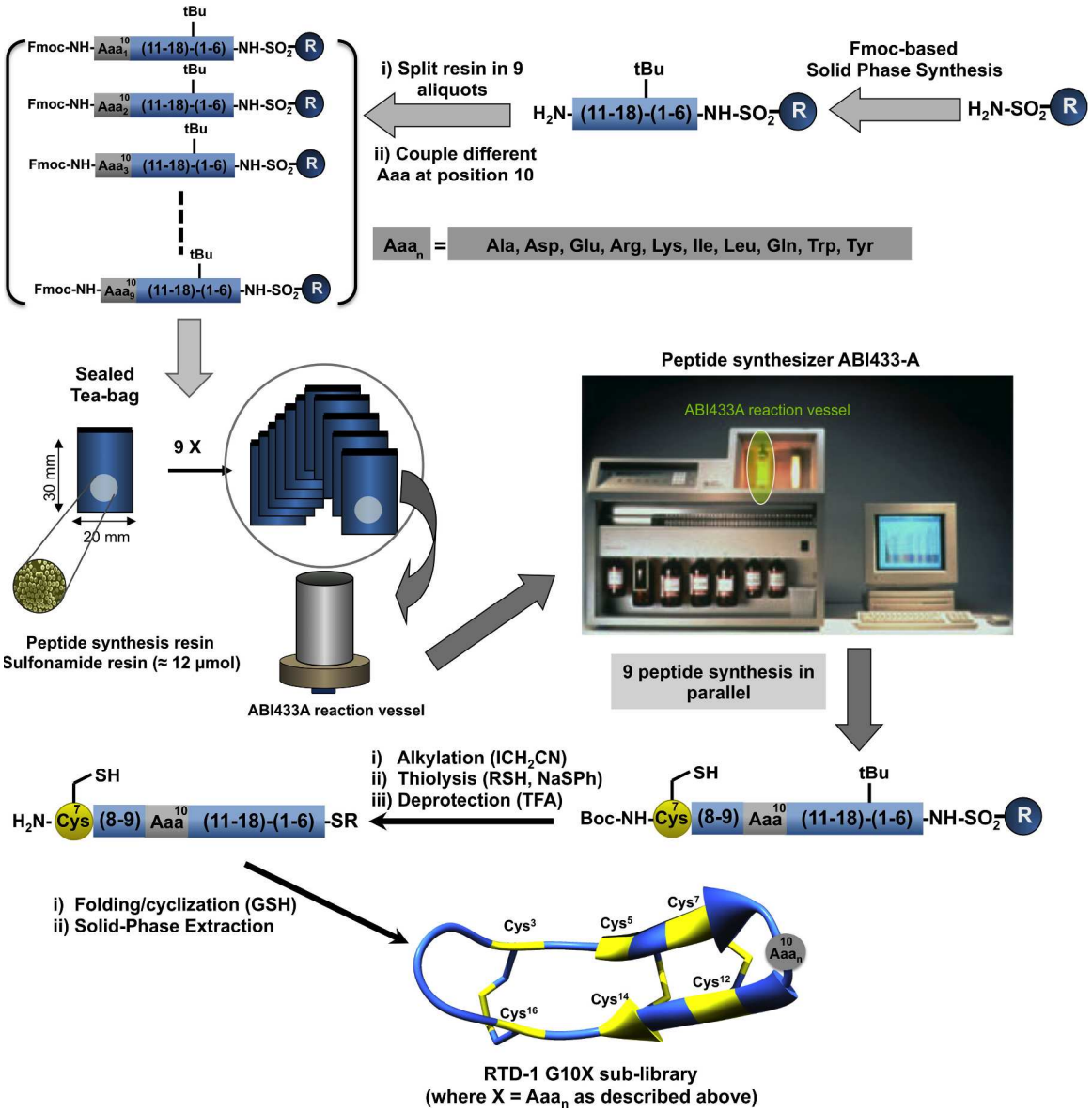

Figure 2. Synthetic scheme used for the parallel production of the amino acid scanning library at position Gly10 of θ-defensin RTD-1 using a 'tea-bag' approach. A similar approach was used for the other positional sub-libraries, except for sub-libraries at positions R4 and L6, where the peptide bond between residues Phe2 and Cys3 was used as the cyclization site.

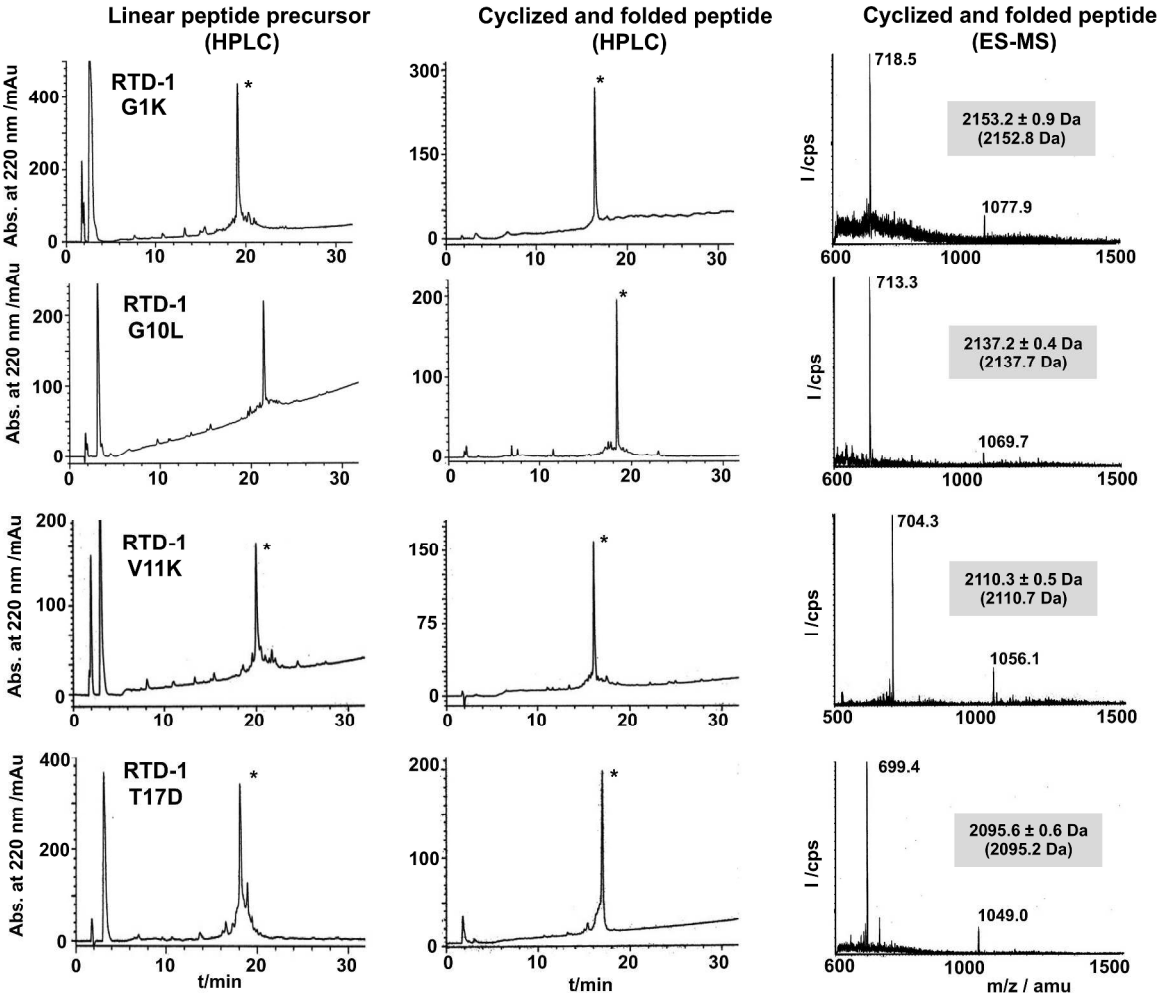

Figure 3. Chemical synthesis and characterization of several single mutant RTD-1 analogs. Analytical HPLC traces of the linear thioester precursor and the GSH-induced cyclization/folding crude after 24 h after desalting to remove buffer components. An asterisk indicates the desired folded peptide (Right panels). ES-MS characterization of the desalted folded/cyclized RTD-1 peptides. The expected average molecular weight is shown in parenthesis (Left panels).

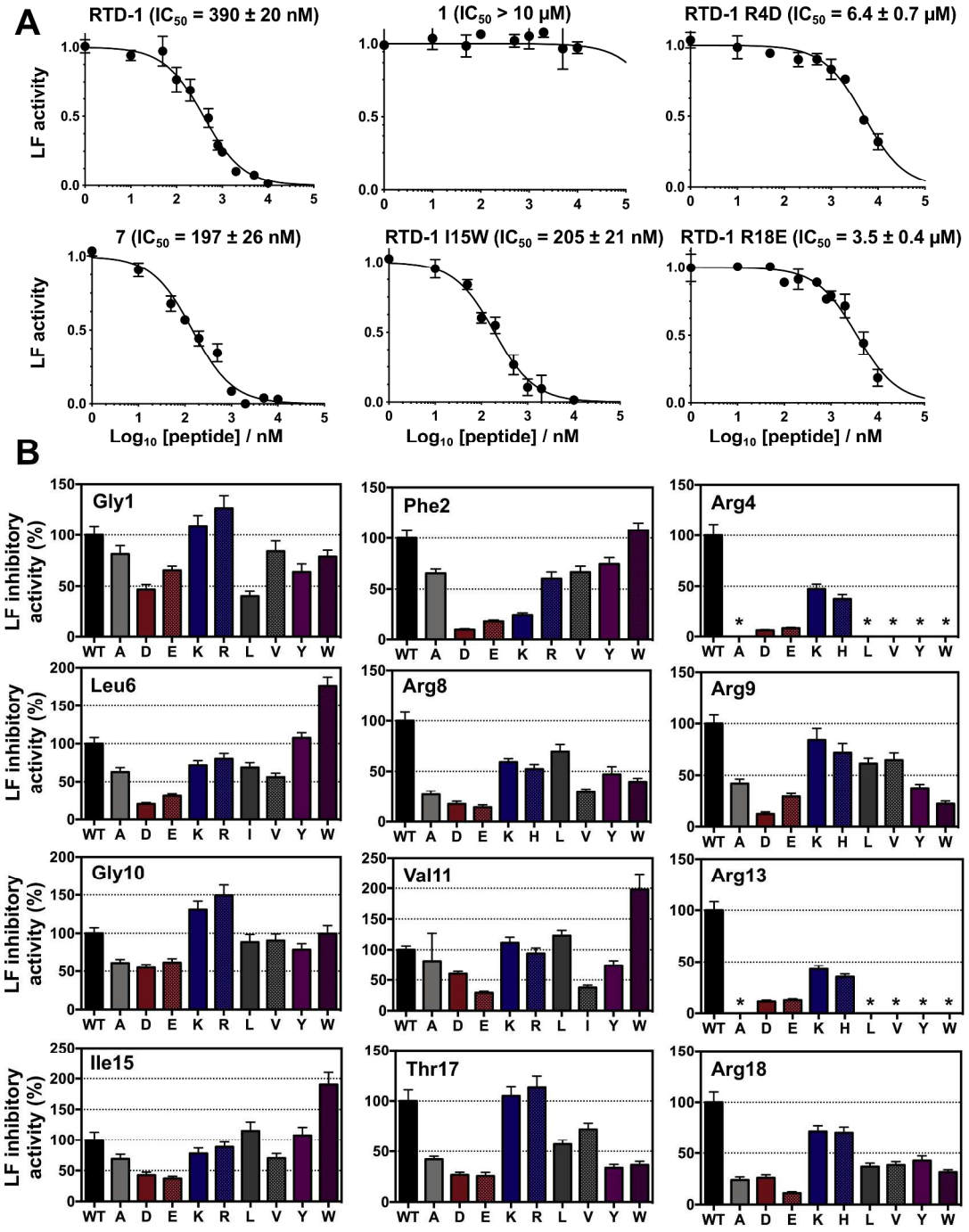

Figure 4. Anti-LF activity for the RTD-1 single mutant analogs. **A.** Dose-dependent inhibition of LF by different single mutant RTD-1 analogs. Peptides RTD-1 and **1** were used a positive and negative controls respectively. **B.** Summary of the relative activities of all single mutants able to provide a folded product. The anti-LF of wild-type RTD-1 was used as a reference, i.e. 100% anti-

LF activity. An asterisk denotes the corresponding mutant was not able to fold efficiently and therefore was not tested for biological activity. Experiments were performed in triplicate (N=3). Error bars indicate standard deviation.

A

Compound	Mutations	IC_{50} (nM)	Relative activity (%)
RTD-1	None, wild-type sequence	390 ± 20	100 ± 6
1	C3S, C5S, C12S, C14S, C16S	>10,000	NA
8	G10R, V11W	125 ± 15	312 ± 37
9	L6W, G10R, V11W	92 ±10	423 ± 46
10	L6W, G10R, V11W, I15W	100 ± 10	392 ± 39
11	F2W, L6W, G10R, V11W, I15W	83 ± 7	473 ± 41
12	G1R, F2W, L6W, G10R, V11W, I15W	61 ± 6	641 ± 60
13	G1R, F2W, L6W, G10R, V11W, I15W, T17R	43 ± 4	914 ± 75

B

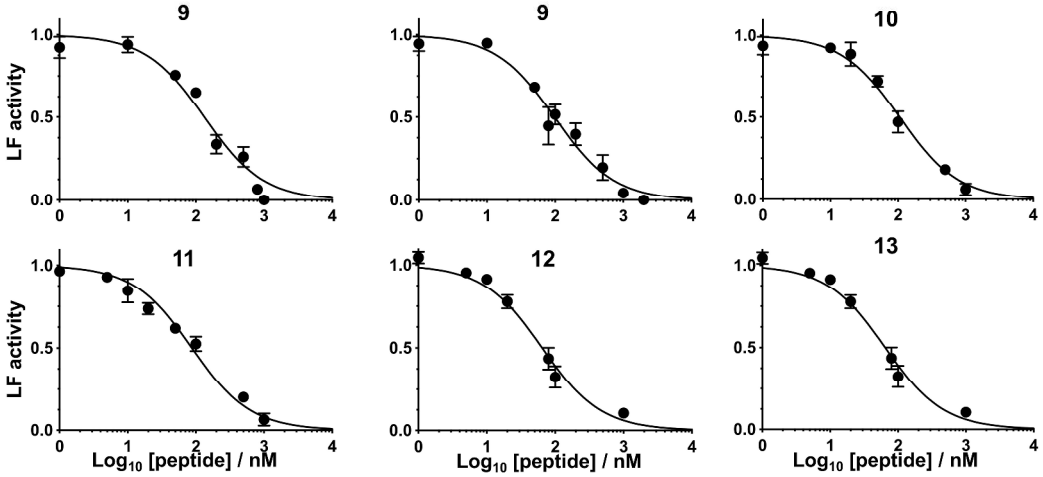

Figure 5. Anti-LF activity of RTD-1 analogs containing multiple mutations, peptide **1** and peptides **8** through **13**. **A.** K_i values and relative activity of the RTD-1 mutants when compared to wild-type RTD-1 is shown at the bottom). Experiments were performed in triplicate (N=3). Error bars indicate standard deviation. NA stands for non active. **B.** Dose-dependent inhibition of LF by different RTD-1 analogs.

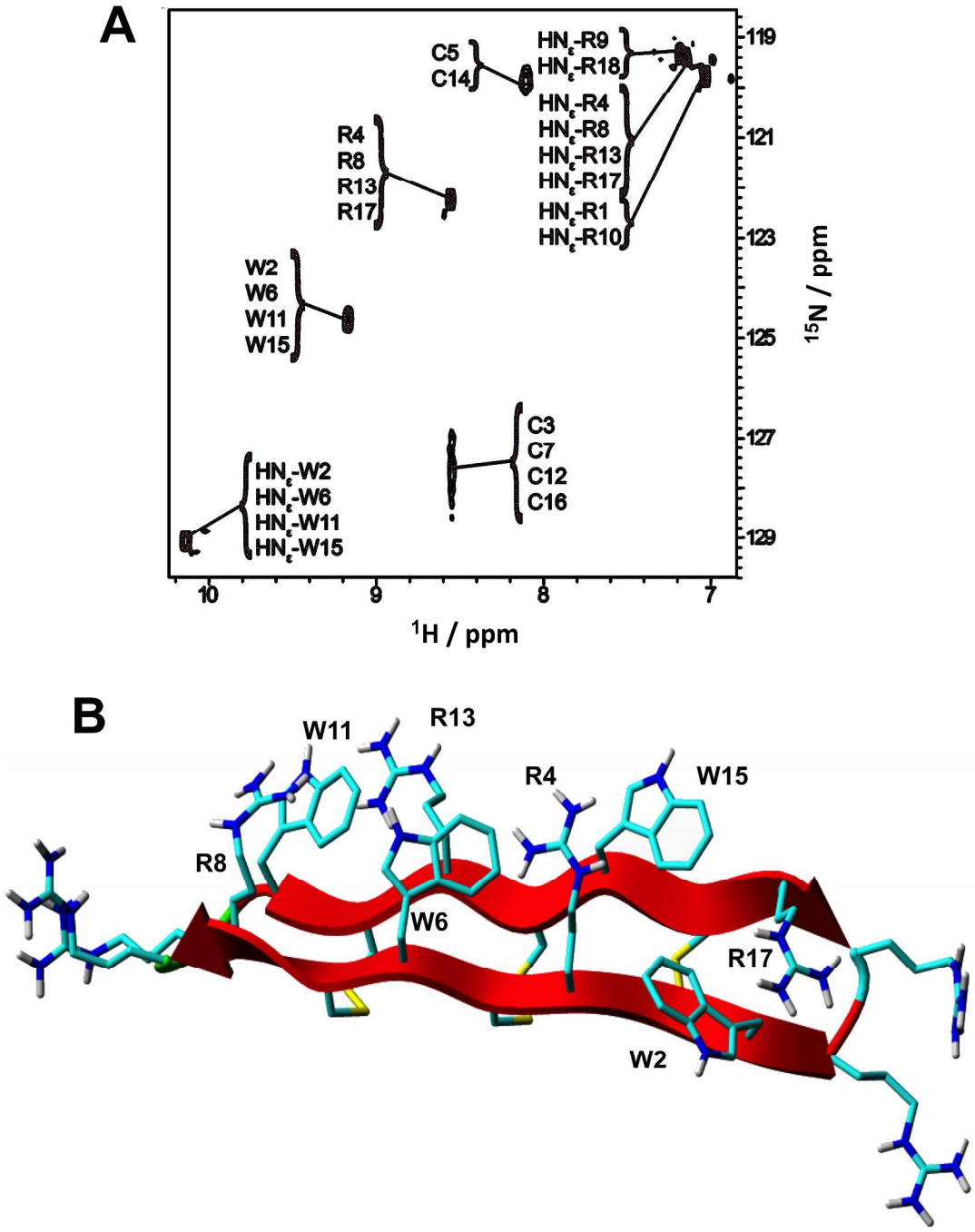

Figure 6. Structural characterization of θ-defensin **13**. **A.** Amide proton and nitrogen peaks in ^{15}N-HSQC of [*U*-15N]-peptide **13** exhibit extreme overlap due to highly symmetric nature of **13** primary structure. Chemical shift assignments of the backbone and side chain amides are indicated. **B.** Homology model of θ-defensin analog **13**. Model was built using the structure of RTD-1 (PDB ID code: 1HVZ)[6] as template. The resulting structure was subjected to molecular

dynamics for 700 ns in a neutral water box containing 0.9% NaCl. One of 10 most stable structures is shown. The structure shows numerous cation-π interactions between the side-chains of different Arg and Trp residues. These interactions were highly dynamic during the simulation (**Fig. S14**) (Graphics were generated using the Yasara software package, www.yasara.org).

Table 1. Inhibitory activity of different RTD-1 mutants against LF and TACE metalloproteases in the presence or absence of bovine serum albumin (BSA).

		0% BSA		0.1% BSA	
Peptide	**Mutations**	**LF protease**	**TACE protease**	**LF protease**	**TACE protease**
		IC_{50} (nM)	**IC_{50} (nM)**	**IC_{50} (nM)**	**IC_{50} (nM)**
RTD-1	none	390 ± 20	4,453 ± 481	1,059 ± 136	ND[a]
2	L6W	221 ± 14	950 ± 118	ND[a]	ND[a]
3	L6D	1,942 ± 152	1,145 ± 147	ND[a]	ND[a]
4	G10R	262 ± 24	870 ± 60	ND[a]	ND[a]
5	G10D	714 ± 56	1,127 ± 148	ND[a]	ND[a]
6	V11I	1041 ± 111	3,857 ± 683	ND[a]	ND[a]
7	V11W	197 ± 26	175 ± 19	ND[a]	3,080 ± 496
8	see Fig. 5A	125 ± 14	672 ± 41	ND[a]	ND[a]
9	see Fig. 5A	92 ± 10	750 ± 50	ND[a]	ND[a]
10	see Fig. 5A	43 ± 4	1,197 ± 151	250 ± 39	≥ 10,000

[a]Not determined

TABLE OF CONTENTS GRAPHIC

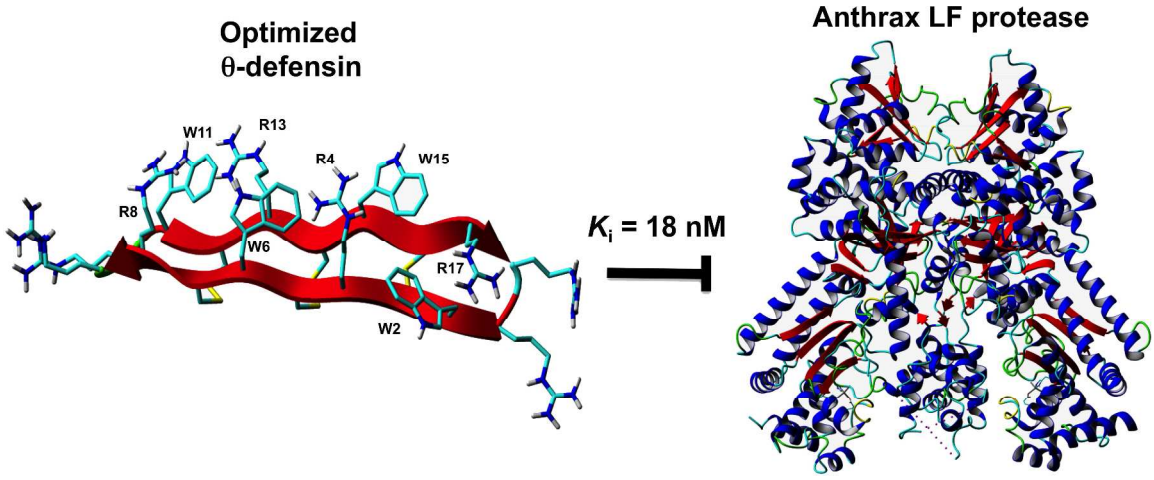

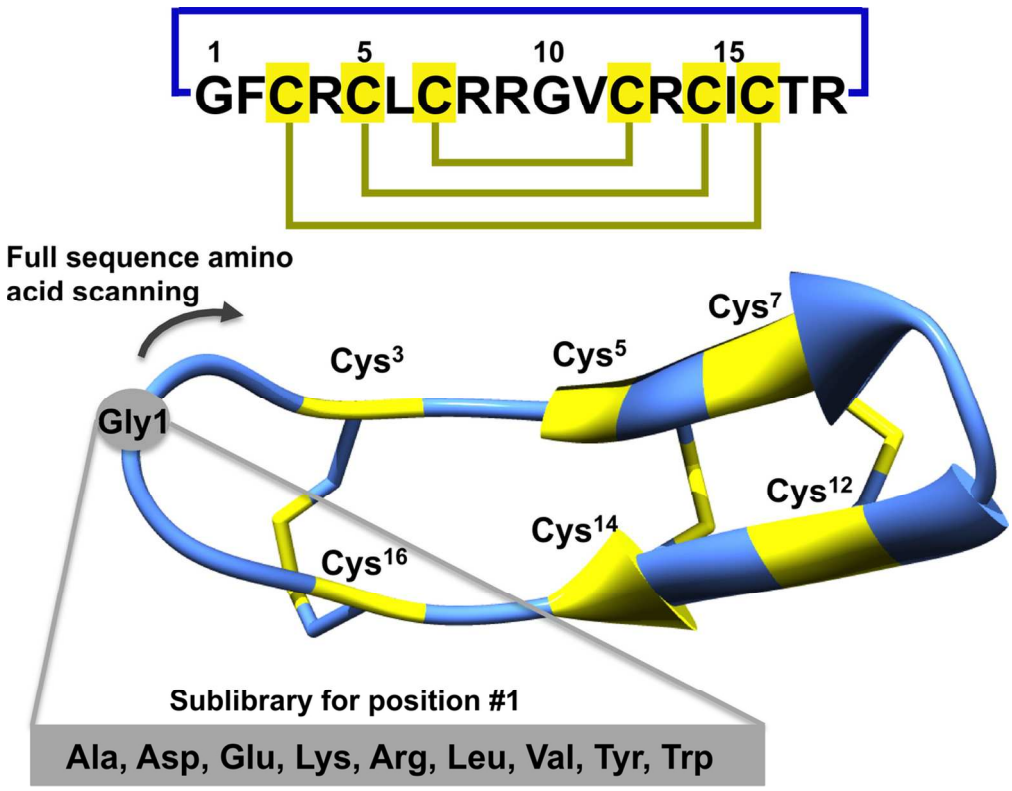

Figure 1. Primary and tertiary structure of rhesus θ-defensin 1 (RTD-1) (PDB ID code: 1HVZ).6 The backbone cyclized peptide (connecting bond shown in blue) is stabilized by the three disulfide bonds in a ladder formation (disulfide bonds shown in yellow). Scheme showing the amino acid scanning approach used in this work. Residues in RTD-1, except for the Cys residues, were replaced by a set of amino acids containing Ala, Asp, Glu, Leu, Val, Lys, Arg, Tyr or Trp. When the native the residue on the RTD-1 sequence was Arg, Leu, or Val, the corresponding amino in the set indicated above was replaced by His (Arg) or Ile (Val and Leu). Also, Leu was not included in the Phe2 sub-library therefore containing only 8 members. Accordingly, a total of 107 (=11 x 9 + 1 x 8) different f RTD-1 variants containing a single mutation were chemically prepared (Table S1).

113x88mm (300 x 300 DPI)

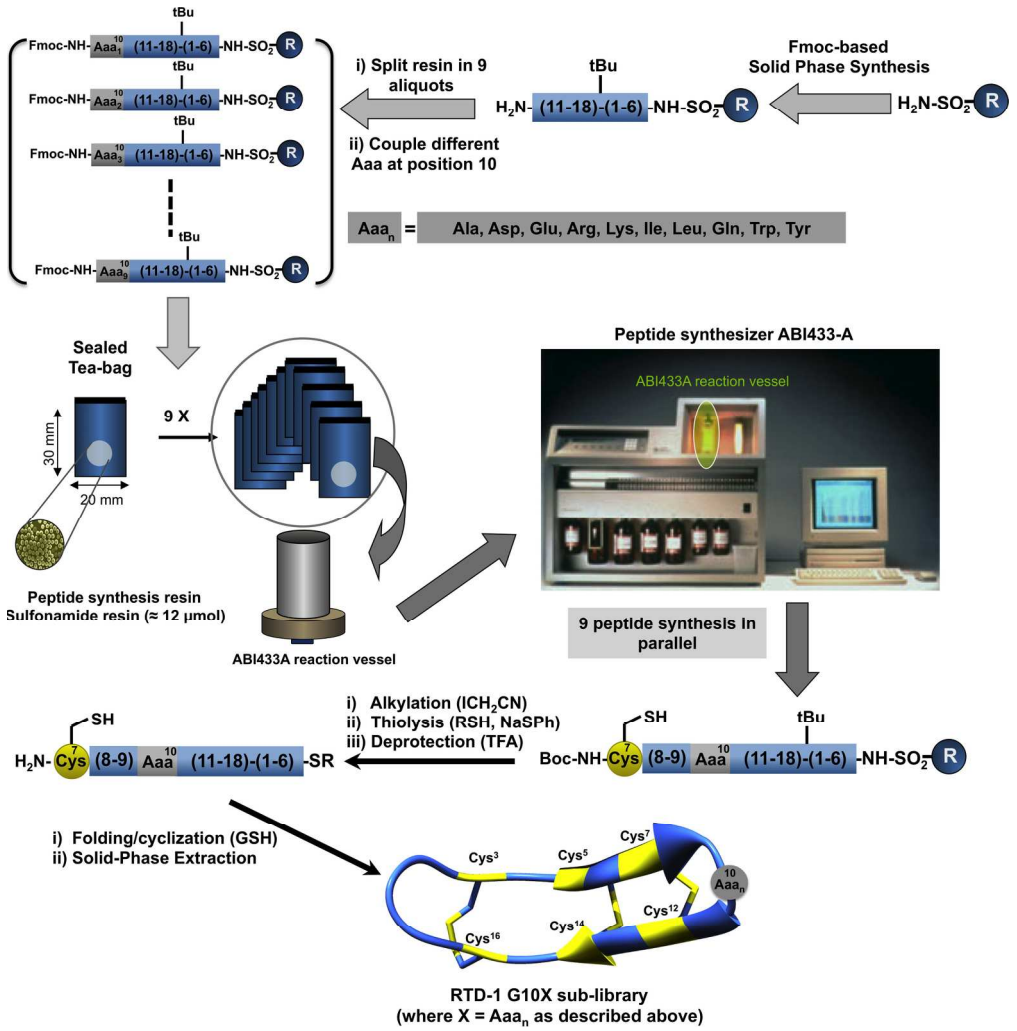

Figure 2. Synthetic scheme used for the parallel production of the amino acid scanning library at position Gly10 of θ-defensin RTD-1 using a 'tea-bag' approach. A similar approach was used for the other positional sub-libraries, except for sub-libraries at positions R4 and L6, where the peptide bond between residues Phe2 and Cys3 was used as the cyclization site.

193x196mm (300 x 300 DPI)

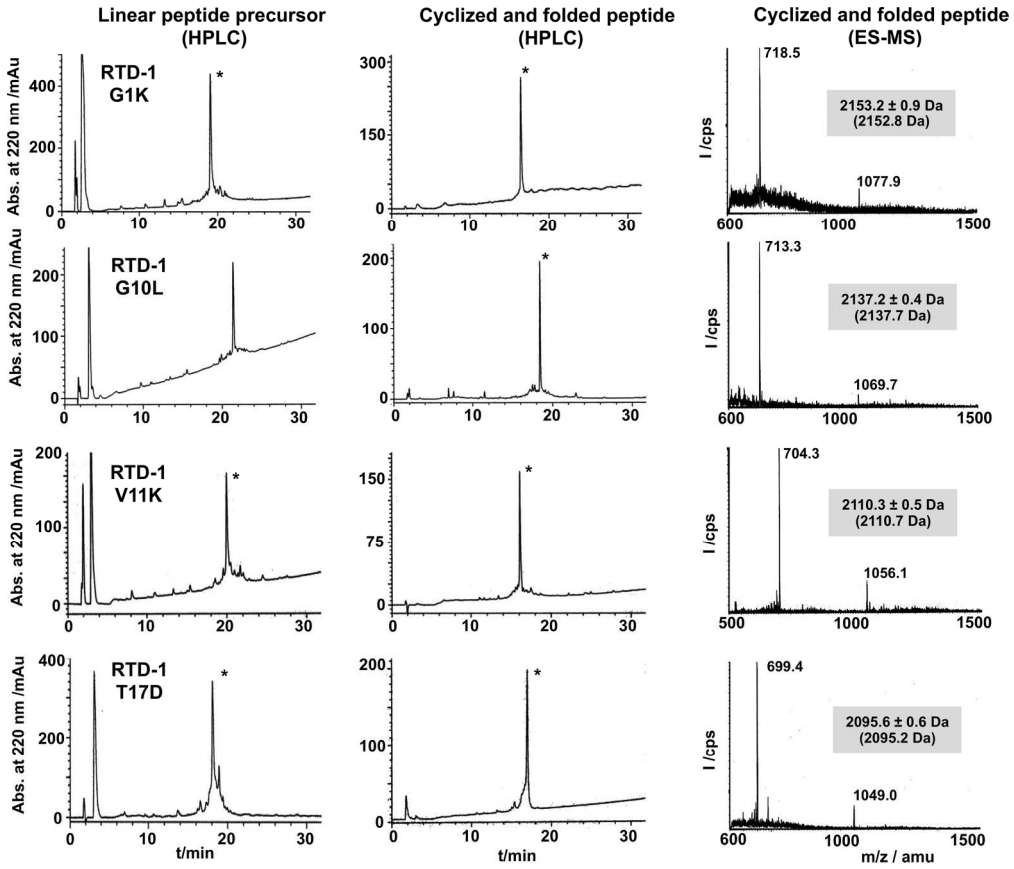

Figure 3. Chemical synthesis and characterization of several single mutant RTD-1 analogs. Analytical HPLC traces of the linear thioester precursor and the GSH-induced cyclization/folding crude after 24 h after desalting to remove buffer components. An asterisk indicates the desired folded peptide (Right panels). ES-MS characterization of the desalted folded/cyclized RTD-1 peptides. The expected average molecular weight is shown in parenthesis (Left panels).

187x160mm (300 x 300 DPI)

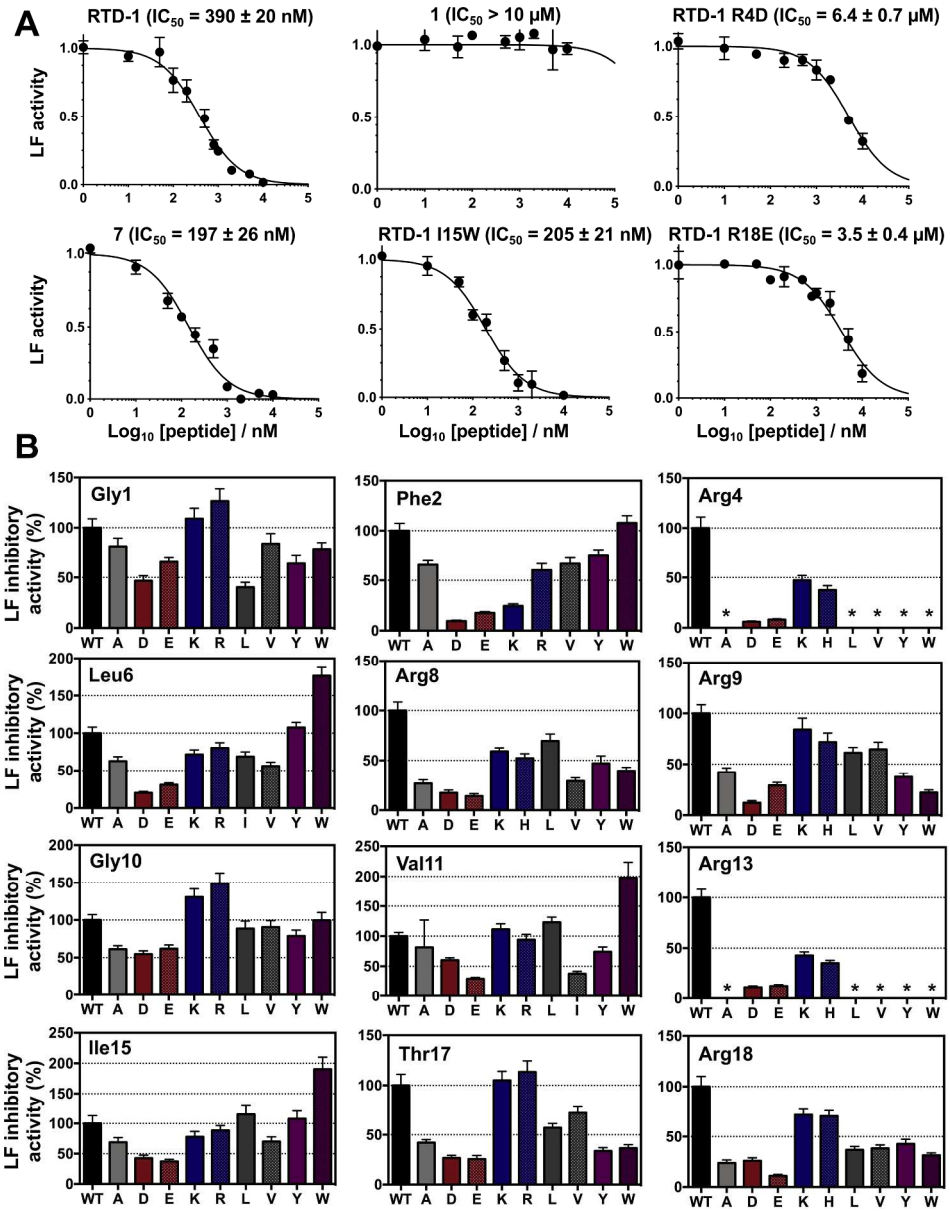

Figure 4

258x328mm (300 x 300 DPI)

A

Compound	Mutations	IC_{50} (nM)	Relative activity (%)
RTD-1	None, wild-type sequence	390 ± 20	100 ± 6
1	C3S, C5S, C12S, C14S, C16S	>10,000	NA
8	G10R, V11W	125 ± 15	312 ± 37
9	L6W, G10R, V11W	92 ±10	423 ± 46
10	L6W, G10R, V11W, I15W	100 ± 10	392 ± 39
11	F2W, L6W, G10R, V11W, I15W	83 ± 7	473 ± 41
12	G1R, F2W, L6W, G10R, V11W, I15W	61 ± 6	641 ± 60
13	G1R, F2W, L6W, G10R, V11W, I15W, T17R	43 ± 4	914 ± 75

B

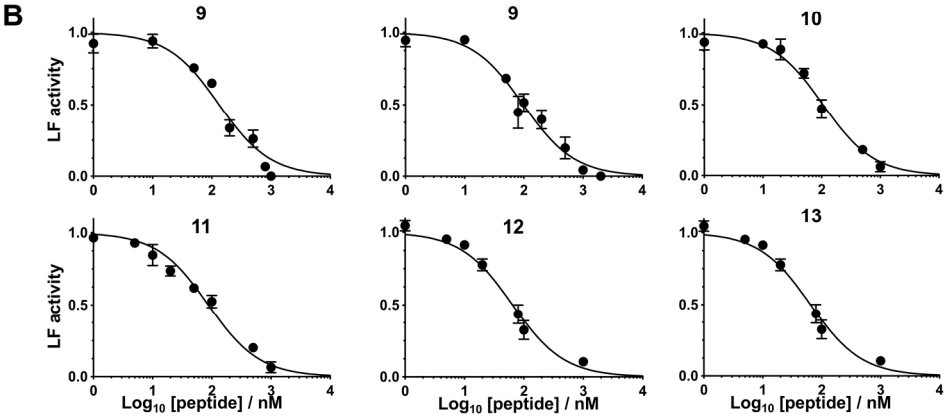

Figure 5

201x161mm (300 x 300 DPI)

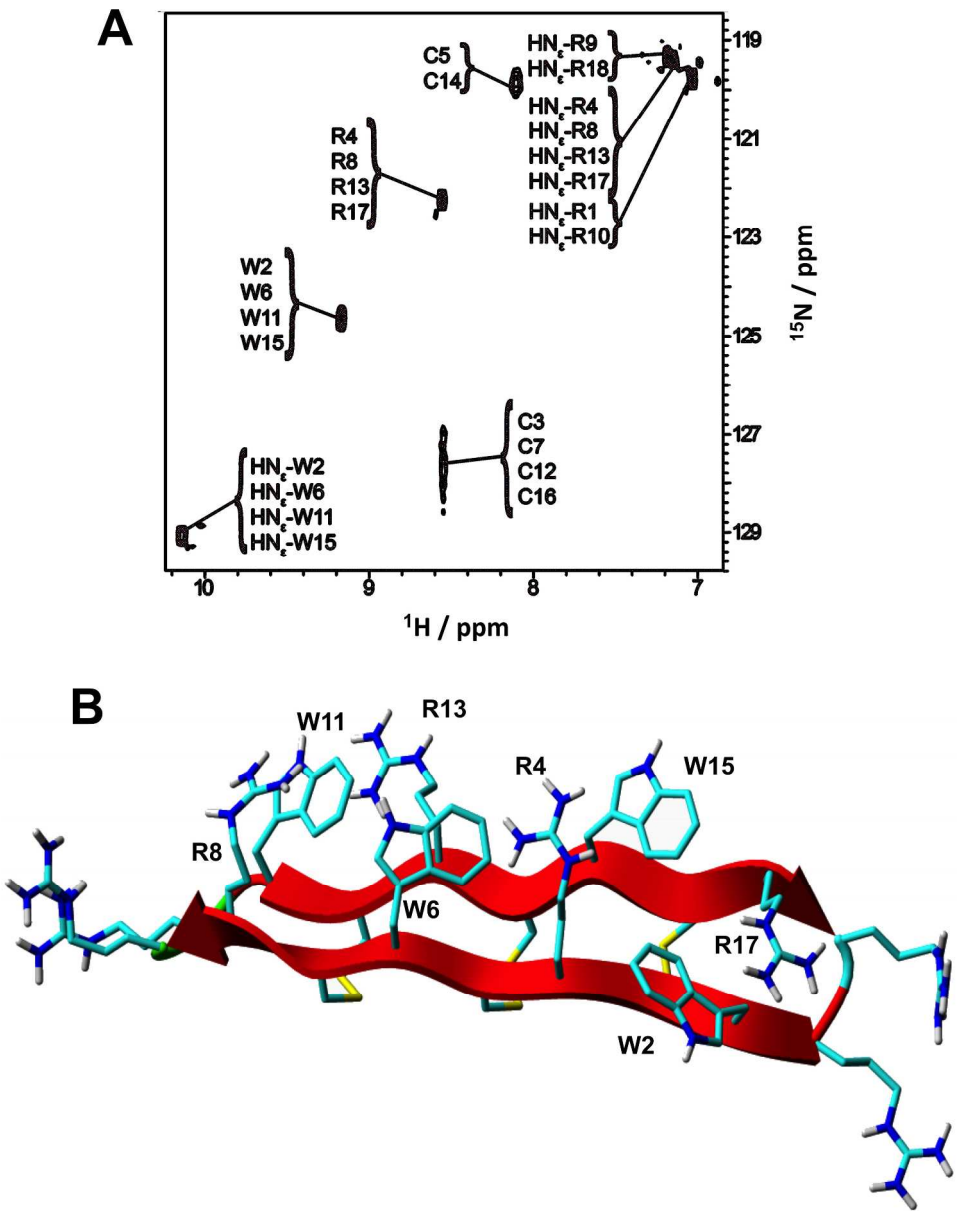

Figure 6. Structural characterization of θ-defensin RTD-1-VI. A. Amide proton and nitrogen peaks in15N-HSQC of [U-15N]-RTD-1-VI exhibit extreme overlap due to highly symmetric nature of RTD-1-VI primary structure. Chemical shift assignments of the backbone and sidechain amides are indicated. B. Homology model of θ-defensin RTD-1-VI. Model was built using the structure of RTD-1 (PDB ID code: 1HVZ)6 as template. The resulting structure was subjected to molecular dynamics for 700 ns in a neutral water box containing 0.9% NaCl. One of 10 most stable structures is shown. The structure shows numerous cation-π interactions between the side-chains of different Arg and Trp residues. These interactions were highly dynamic during the simulation (Fig. S14) (Graphics were generated using the Yasara software package, www.yasara.org).

239x300mm (300 x 300 DPI)

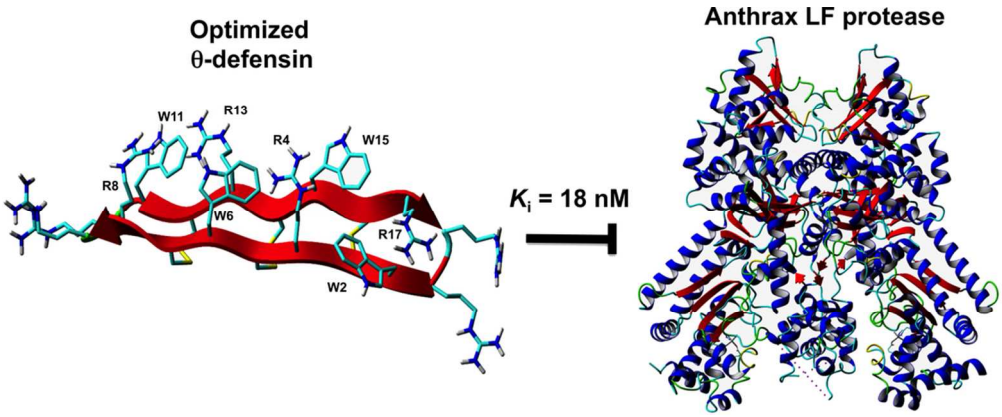

TOC

98x40mm (300 x 300 DPI)